145 (2023) 213238

Contents lists available at ScienceDirect

Biomaterials Advances

journal homepage: www.journals.elsevier.com/materials-science-and-engineering-c

Tailored anti-biofilm activity – Liposomal delivery for mimic of small antimicrobial peptide

Lisa Myrseth Hemmingsen [a], Barbara Giordani [b], Marianne H. Paulsen [c,d], Željka Vanić [e], Gøril Eide Flaten [a], Beatrice Vitali [b], Purusotam Basnet [f], Annette Bayer [c], Morten B. Strøm [d], Nataša Škalko-Basnet [a,*]

[a] Drug Transport and Delivery Research Group, Department of Pharmacy, University of Tromsø The Arctic University of Norway, Universitetsvegen 57, N-9037 Tromsø, Norway
[b] Beneficial Microbes Research Group, Department of Pharmacy and Biotechnology, University of Bologna, Via San Donato 19/2, 40127 Bologna, Italy
[c] Department of Chemistry, University of Tromsø The Arctic University of Norway, Universitetsvegen 57, N-9037 Tromsø, Norway
[d] Natural Products and Medicinal Chemistry Research Group, Department of Pharmacy, University of Tromsø The Arctic University of Norway, Universitetsvegen 57, N-9037 Tromsø, Norway
[e] Department of Pharmaceutical Technology, Faculty of Pharmacy and Biochemistry, University of Zagreb, A. Kovačića 1, 10 000 Zagreb, Croatia
[f] Women's Health and Perinatology Research Group, Department of Clinical Medicine, University of Tromsø The Arctic University of Norway, Universitetsveien 57, N-9037 Tromsø, Norway

ARTICLE INFO

Keywords:
Peptidomimetics
Liposomes
Bacterial biofilms
Membrane-active antimicrobials
Chronic wounds

ABSTRACT

The eradication of bacteria embedded in biofilms is among the most challenging obstacles in the management of chronic wounds. These biofilms are found in most chronic wounds; moreover, the biofilm-embedded bacteria are considerably less susceptible to conventional antimicrobial treatment than the planktonic bacteria. Antimicrobial peptides and their mimics are considered attractive candidates in the pursuit of novel therapeutic options for the treatment of chronic wounds and general bacterial eradication. However, some limitations linked to these membrane-active antimicrobials are making their clinical use challenging. Novel innovative delivery systems addressing these limitations represent a smart solution. We hypothesized that incorporation of a novel synthetic mimic of an antimicrobial peptide in liposomes could improve its anti-biofilm effect as well as the anti-inflammatory activity. The small synthetic mimic of an antimicrobial peptide, 7e-SMAMP, was incorporated into liposomes (~280 nm) tailored for skin wounds and evaluated for its potential activity against both biofilm formation and eradication of pre-formed biofilms. The 7e-SMAMP-liposomes significantly lowered inflammatory response in murine macrophages (~30 % reduction) without affecting the viability of macrophages or keratinocytes. Importantly, the 7e-SMAMP-liposomes completely eradicated biofilms produced by *Staphylococcus aureus* and *Escherichia coli* above concentrations of 6.25 μg/mL, whereas in *Pseudomonas aeruginosa* the eradication reached 75 % at the same concentration. Incorporation of 7e-SMAMP in liposomes improved both the inhibition of biofilm formation as well as biofilm eradication *in vitro*, as compared to non-formulated antimicrobial, therefore confirming its potential as a novel therapeutic option for bacteria-infected chronic wounds.

Abbreviations: AMP, antimicrobial peptide; AMR, antimicrobial resistance; B3M-liposomes, Bacterial Membrane-Mimic Liposomes Model; CCK-8, cell counting kit-8; CFU, colony-forming unit; DMEM-hg, Dulbecco's Modified Eagle Medium high glucose; DMSO, dimethyl sulfoxide; EE, entrapment efficiency; FBS, fetal bovine serum; FITC, fluorescein isothiocyanate; HEPES, N-(2-hydroxyethyl)piperazine-N′-(2-ethanesulfonic acid); LPS, lipopolysaccharide; MAAs, membrane-active antimicrobials; MBC, minimum bactericidal concentration; MDR, multidrug-resistant; MIC, minimal inhibiting concentration; mQ, milli-Q water; M_w, molecular weight; NB, nutrient broth; PBS, phosphate buffered saline; PI, polydispersity index; RPMI, Roswell Park Memorial Institute; SMAMP, synthetic mimics of antimicrobial peptide; SWF, simulated wound fluid; TEM, transmission electron microscopy.

* Corresponding author.
E-mail address: natasa.skalko-basnet@uit.no (N. Škalko-Basnet).

https://doi.org/10.1016/j.bioadv.2022.213238
Received 24 August 2022; Received in revised form 18 November 2022; Accepted 6 December 2022
Available online 13 December 2022

1. Introduction

As we are entering a post-antibiotic era, antimicrobial resistance (AMR) has become one of the major medical concerns and critical hurdles in medical care, often with fatal consequences [1]. Over the course of time, the inevitable rise of AMR and multidrug-resistant (MDR) pathogens have rendered many infections practically untreatable and potentially life threatening. Moreover, researchers struggle to bring forward novel antimicrobial compounds for new targets, resulting in the clinical pipelines for antimicrobial compounds being rather stagnant [2]. With this upsurge of AMR and limited arsenal of antimicrobial compounds and therapeutic options, chronic wounds and wound management are rapidly growing challenges for both patients and health care providers. Furthermore, due to an aging population and increased prevalence of diabetes and obesity, cases of chronic wounds are increasing and expected to further rise [3]. Amid these challenges of chronic wound treatment, it is essential to focus on biofilms as they are found in up to 80 % of all chronic wounds [4]. Bacteria embedded in these bacterial communities often have 1000-fold increased tolerance to antibiotics. Moreover, there are no antimicrobials specifically targeting biofilm eradication approved by the major regulatory agencies [5,6]. Antimicrobial peptides (AMPs) are often considered promising candidates to mitigate the effects and progression of AMR [7,8]. The antimicrobial activities of AMPs and other membrane-active antimicrobials (MAAs) reach beyond disruption of bacterial membranes. For instance, many cause alterations of immune responses as well as target the internal components, such as DNA, in bacteria [9,10]. Besides, AMPs have proven to evoke less resistance due to their fast onset of action and activity against metabolically inactive bacteria [11]. The antimicrobial activity of AMPs is often broad, including gram-positive and gram-negative bacteria, viruses, and fungi [12,13]. Additionally, AMPs and other MAAs could improve the eradication of biofilm-embedded bacteria compared to the more conventional antimicrobials [6].

All listed properties bear optimism around AMPs as valuable candidates in the path to ease the challenges around AMR and eradication of biofilm-embedded bacteria; however, some frequent general drawbacks linked to AMPs require careful consideration. These limitations include their toxicity, haemolytic activity, loss of *in vivo* efficacy, and proteolytic instability [7,11]. These are among the most common reasons for their discontinuation before or in early-stage clinical trials [9]. Researchers have tried to evade these problems, further improving the therapeutic index, by chemically modifying AMPs or creating AMP mimics. A fine-tuned balance between activity and toxicity or selectivity is vital for the success of these compounds [14]. Development of peptidomimetics or synthetic mimics of antimicrobial peptides (SMAMPs) could overcome the hurdles of instability, lowered bioavailability, and immunogenicity [15]. Although small SMAMPs are especially promising drug candidates, some of the issues considering clinical settings remain, namely, interactions with biomolecules, tendencies to proteolytic degradation, toxicity, and rather low *in vitro/in vivo* translation. The remaining issues limit their clinical applicability as well as faster progress in the pipelines [14,16].

Pursuing topical administration routes such as efficient localized therapy of skin and vaginal infections could help circumvent many of the SMAMPs limitations linked to systemic route; however, certain obstacles remain to be addressed even for topical routes [14]. Drug delivery strategies, using *e.g.*, nanomaterials, could advance the therapeutic index and increase exposure or contact time and retention at the infected area [8,17,18]. Lipid-based systems for MAA delivery have previously demonstrated superior antimicrobial activity and could therefore be suitable alternatives for the delivery of these compounds [7,19,20]. We have previously established that liposomes associated with MAA chlorhexidine improved biofilm eradication in addition to lower inflammatory responses in macrophages [21]. Moreover, liposomes can facilitate sustained release of the active compound which in turn could lower the risk of bacterial regrowth, improve interaction with the bacterial membrane, and increase the exposure time [17,22]. Additionally, liposomes enable accumulation of the active compound at the infected site, thus limiting systemic exposure due to their ability to interact with skin lipids, making them suitable for topical skin administration [23,24]. Even though formulated and non-formulated AMPs and their mimics are well-studied for their potential in microbial eradication, there are few studies dealing with biofilms related to wounds, moreover, many of the studies on AMPs associated with liposomes investigated their potential as food preservatives [6,14,25]. However, we believe that the SMAMPs combined with liposomes could primarily serve as a therapeutic option for treating biofilm-infected chronic wounds.

In the present study, 7e-SMAMP, a novel SMAMP with excellent antimicrobial properties [15], was incorporated into liposomes optimized for treatment of biofilm-infected chronic skin wounds. Development of 7e-SMAMP was inspired by incorporating important properties of AMPs into a cationic and amphipathic scaffold mimicking the marine antimicrobials *Eusynstyelamides* found in bryozoan *Tegella cf. spitzbergensis* [15]. We hypothesized that associating the membrane-active 7e-SMAMP with liposomes could improve *in vitro* biofilm eradication of bacteria commonly found in wounds in addition to lowering the inflammatory activity of macrophages therefore further improving healing. After initial optimization and characterization of 7e-SMAMP-liposomes, the evaluation of *in vitro* performance of the delivery system focused on cell compatibility, anti-inflammatory properties, and antimicrobial efficacy.

2. Experimental section

2.1. Materials

Lipoid S100 (phosphatidylcholine content >94 %) was kindly provided by Lipoid GmbH (Ludwigshafen, Germany). Methanol (≥99.9 %), HiPerSolv CHROMANORM® for LC-MS, acetonitrile (≥99.9 %), HiPerSolv CHROMANORM®, gradient grade for HPLC and acetic acid (>99.9 %) were purchased from VWR International (Fontenay-sous-Bois, France). Phosphoric acid (>85 %) was acquired from Kebo lab (Oslo, Norway). Albunorm (200 mg/mL human serum albumin) was acquired from Octapharma AG (Lachen, Switzerland). Sepharose™ CL-4B was purchased from GE Healthcare (Uppsala, Sweden). 1,2-Dioleoyl-*sn*-glycero-3-phospho-*rac*-(1-glycerol) (DOPG), and 1-palmitoyl-2-(6-[(7-nitro-2-1,3-benzoxadiazol-4-yl)amino]hexanoyl)-*sn*-glycero-3-[phospho-*rac*-(1-glycerol)] (ammonium salt) (C_6-NBD-PG) were obtained from Avanti Polar Lipids (Alabaster, AL, USA). 1,2-Dioleoyl-*sn*-glycero-3-phosphoethanolamine (DOPE) was obtained from Lipoid GmbH (Ludwigshafen, Germany). Trifluoroacetic acid (TFA) for HPLC (≥99.0 %), chloroform (99.0–99.4 %, GC), glycerol solution (86–89 %), sodium phosphate dibasic dihydrate, potassium phosphate monobasic, sodium chloride, EDTA sodium, sodium hydrogen carbonate, potassium chloride, calcium chloride dehydrate, cardiolipin sodium salt from bovine heart (≥97 %), N-(2-Hydroxyethyl)piperazine-N′-(2-ethanesulfonic acid) (HEPES), sodium dithionite, fluorescein isothiocyanate–dextran average molecular weight (M_w) 3000–5000 Da (FITC–dextran 4400), fluorescein isothiocyanate–dextran average M_w 20,400 Da (FITC–dextran 20,400), Kollisolv® PEG E 400, Phospholipid Assay Kit for colorimetric or fluorometric tests, N-(−1-Naphthyl)ethylenediamine dihydrochloride, sulphanilamide, Triton™ X-100, and Cell Counting Kit-8 (CCK-8) were purchased from Sigma-Aldrich (St. Louis, MO, USA). Penicillin-streptomycin (10,000 units/mL and 10 mg/mL, respectively), lipopolysaccharides (LPS) from *Escherichia coli* O55:B5, RPMI-1640 medium (with L-glutamine and sodium bicarbonate) and fetal bovine serum (FBS) were obtained from Sigma-Aldrich (Steinheim, Germany). Dulbecco's Modified Eagle Medium high glucose (DMEM-hg) w/L-glutamine and sodium pyruvate was purchased from Biowest (Nuaillé, France). Nutrient Broth (NB) was supplied by Becton Dickinson and Company (Sparks, MD, USA). Murine macrophage, RAW 264.7 cell line

was obtained from ATCC (Manassas, VA, USA). HaCaT cell line (immortalized human keratinocytes) was purchased from CLS Cell Lines Service GmbH (Eppelheim, Germany). *Staphylococcus aureus* ATCC29213, *Escherichia coli* ATCC11105, *Pseudomonas aeruginosa* ATCC10145 were purchased from American Tissue and Cell Culture Corp. (Manhasset, Virginia, USA). *Staphylococcus aureus* SO2, SO83, SO86, and SO88 are clinical isolates (Ospedale Sant'Orsola-Malpighi, Bologna, Italy) [26].

2.2. SMAMP synthesis

The synthesis of the 7e-SMAMP (Fig. 1) has been previously described by Paulsen et al. including the detailed methodology and materials involved [15]. However, a brief overview of the procedure is provided in Supplementary Material (S1.1.).

2.3. Evaluation of 7e-SMAMP stability

The 7e-SMAMP stock solutions were diluted to 25 and 50 μM with simulated wound fluid (SWF; 5.84 g/L NaCl, 3.36 g/L $NaHCO_3$, 0.3 g/L KCl, 0.35 g/L $CaCl_2 \cdot 2H_2O$, and 33 g/L albumin from Albunorm in milli-Q water (mQ)) [27] or mQ and analysed using reversed-phase chromatography [28] with a Waters e2795 separations module combined with a Waters 2489 UV–VIS detector. The quantification of 7e-SMAMP was carried out using Waters XBridge® C18 column (5 μm, 4.6 × 250 mm) and a Waters XBridge® C18 guard cartridge (5 μm, 4.6 × 20 mm, Waters Corporation, Milford, CT, USA) modified from a method by Paulsen et al. [29]. The 7e-SMAMP was eluted with mobile phases comprising mQ and acetonitrile, both with TFA (0.1 %, *v*/v). The gradient starting at 50 % acetonitrile followed a linear gradient to 75 % acetonitrile over 8 min with a flow of 1 mL/min at detection wavelength set to 231 nm.

Prior to the evaluation of 7e-SMAMP stability, we performed a UV-VIS scan analysis [28]; the detailed procedure can be found in Supplementary Materials (S1.2.). All solutions were stored for 7 days at 4, 25, and 32 °C. Chemical evaluations of stability were performed at preparation time and after 1- and 7-days storage.

2.4. Liposome preparation and size reduction

The thin film method was utilized to prepare liposomes. In short, Lipoid S100 (200 mg) and 7e-SMAMP (20 mg) were dissolved in 10 mL methanol. Lipid films were created by evaporation on Büchi rotavapor R-124 (equipped with vacuum controller B-721, Büchi Vac® V-500 and Büchi B-480 water bath, Büchi Labortechnik, Flawil, Switzerland) at 60 mBar and 45 °C for at least 1 h. The lipid film was rehydrated with 10 mL distilled water to form liposomes. Empty liposomes (without 7e-SMAMP) were prepared with only Lipoid S100 in the lipid film. The size of the liposomes was reduced by manual extrusion through polycarbonate membranes (Nuclepore Track-Etch Membrane, Whatman House, Maidstone, UK). The size reduction was achieved by successional manual extrusion through 0.8 μm (three times), 0.4 μm (five times), and 0.2 μm (two times) membranes [21].

2.5. Liposome characterization - size, zeta potential, pH, and entrapment efficiency determination

The liposome size was determined with a Malvern Zetasizer Nano Zen 2600 (Malvern, Oxford, UK). The liposomes were diluted 1:100 (*v*/v) with 0.2 μm filtered tap water prior to every measurement and measured in triplicates.

The zeta potential was determined with the Zetasizer Nano Zen 2600 (Malvern, Worcestershire, UK). The liposomes were diluted 1:20 (v/v) in 0.2 μm filtered tap water prior to every measurement and measured in triplicates.

The pH was determined using the Accumet®, Portable pH meter AP115 (Fisher Scientific, MA, USA) at room temperature (21 ± 1 °C). The stability of the 7e-SMAMP-liposomes was evaluated, and the procedure is described in the Supplementary Materials (S1.3.).

Liposomes were dialyzed (tube, MWCO: 12–14 kDa; Spectra/Por®4, Spectrum®, VWR International, Fontenay-sous-Bois, France) for 4 h (1:1000, *v*/v) as previously described [21]. HPLC was utilized to determine 7e-SMAMP concentrations as described in Section 2.3.

2.6. Morphology studies by transmission electron microscopy

The morphology of 7e-SMAMP-liposomes was investigated using transmission electron microscopy (TEM) as reported earlier [30]. Liposomes were deposited onto carbon-coated grids and stained with 3 % uranyl acetate and 2 % methylcellulose. The images were acquired with microscope HT7800 Series (Hitachi High-Tech Corp., Tokyo, Japan) at an accelerated voltage of 100 kV coupled with a Morada camera.

2.7. Phospholipid content of liposomes

The phospholipid content of liposomes was measured with Phospholipid Assay Kit according to the technical bulletin provided by the supplier. Prior to the experiment, liposomes (50 μL) were diluted with distilled water to a total volume of 10 mL. Finally, the phospholipid content was measured on a UV–VIS plate reader (Tecan Trading AG, Männedorf, Switzerland) at 570 nm.

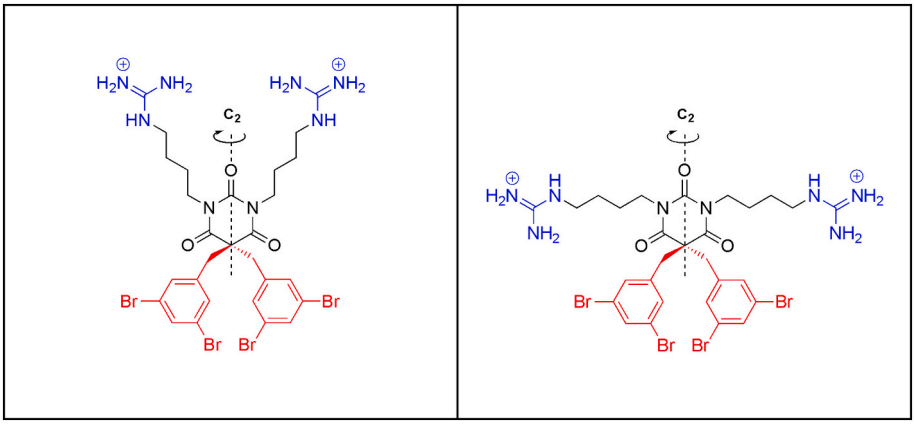

Fig. 1. Structure of the 7e-SMAMP. The barbiturate ring ensures an amphipathic and achiral scaffold with C_2-symmetry.

2.8. Elasticity of liposomal membranes

The assessment of the elasticity of the liposomal membranes to confirm integrity of liposomes followed a method by Palac et al. [31]. The empty and 7e-SMAMP-liposomes were extruded with a constant pressure of 2.5 Bar through a membrane with a pore size of 100 nm. The amount of liposomal suspension passing through the membrane within 5 min and liposomal mean diameter were recorded. Empty liposomes served as control for 7e-SMAMP-liposomes. The elasticity was calculated according to Eq. (1):

$$E = J \times \left(r_v / r_p\right)^2 \quad (1)$$

where J represents the amount (g) of liposomal suspension passing through the membrane within 5 min, r_v represents mean diameter (nm) after extrusion, and r_p represents pore size of the membrane (nm).

2.9. In vitro release studies

The *in vitro* 7e-SMAMP release from the liposomes was evaluated using tubes of pre-soaked regenerated cellulose (MWCO: 12–14 kDa) membranes (Spectra/Por®4, Spectrum®, VWR International, Fontenay-sous-Bois, France) [32]. The medium (150 mL) used in the experimental setup was PEG E400 (10 %, *v*/v) in distilled water, heated to 32 °C. An aliquot (1.5 mL) of 7e-SMAMP-liposomes or 7e-SMAMP dissolved in acceptor medium was added to the dialysis membrane. Samples were withdrawn after 1, 2, 3, 4, 6, 8, and 24 h and analysed using HPLC as described in Section 2.3. The sample volume was replaced with fresh medium in the acceptor phase after every sampling. The sink conditions were assured. The cumulative release of formulated and non-formulated 7e-SMAMP (applied at the same concentration) was compared.

2.10. Evaluation of cell viability

AMPs and their mimics often display certain level of toxicity to eukaryotic cells; therefore, to ensure the safety of the novel formulations we evaluated cytotoxicity using Cell counting kit – 8 (CCK-8) as described previously [33]. Suspensions of HaCaT or RAW 264.7 cells (90 μL, 1 × 10^5 cells/mL) were plated on 96-well plates and incubated for 24 h (37 °C/5 % CO_2). The macrophages were cultured in complete RPMI (containing 10 % FBS, penicillin-streptomycin), while keratinocytes were cultured in complete DMEM-hg (containing 10 % FBS, penicillin-streptomycin). The pre-incubated cells were treated with 10 μL of medium (control), diluted liposome suspensions (1, 10, and 50 μg/mL lipid concentration) and incubated for another 24 h (37 °C/5 % CO_2). An aliquot of 10 μL CCK-8 reagent was added to each well and the cells were incubated for 4 h (37 °C/5 % CO_2, total incubation of 28 h). To evaluate the cell survival, the cells were assessed using a UV–VIS plate reader (Tecan Trading AG, Männedorf, Switzerland) at 450 nm and referenced at 650 nm. The results were expressed as percentage of surviving cells compared to the non-treated cells (control). Three batches for each formulation were tested in triplicates.

2.11. Assessment of anti-inflammatory activity

Anti-inflammatory activities of empty and 7e-SMAMP-liposomes were determined by assessing lipopolysaccharide (LPS)-induced nitric oxide (NO) production in murine macrophages. Macrophages (RAW 264.7) were cultured in complete RPMI and seeded in 24-well plates (1 mL, 5 × 10^5 cells/mL) prior to incubation (37 °C/5 % CO_2) for 24 h. After incubation, the complete medium was replaced with medium containing LPS (1 μg/mL). The cells were then treated with liposomal suspensions (1, 10, and 50 μg/mL lipid concentration). The LPS containing medium and complete medium served as controls. The cells were then incubated for another 24 h and NO production evaluated on a UV–VIS plate reader (Tecan Trading AG, Männedorf, Switzerland) with Griess reagent (1:1, *v*/v; 2.5 % phosphoric acid with 1 % sulphanilamide and 0.1 % N-(−1-naphthyl)ethylenediamine) at 540 nm [33]. Three batches for each formulation were tested in triplicates.

2.12. Effects of 7e-SMAMP on bacterial membrane-mimic liposomes model

2.12.1. Bacterial membrane-mimic liposomes model

Bacterial Membrane-Mimic Liposomes Models (B3M-liposomes) mimicking *S. aureus* membranes were tailored according to literature [34,35]. In brief, DOPG and cardiolipin (20 mg) were dissolved in chloroform and methanol (2:1, *v*/v) in a molar ratio of 58:42. A lipid film was produced by solvent evaporation on a rotary evaporator at 45 °C, 60 mBar, and 60 rpm for 2 h to remove the solvents. The lipid films were rehydrated with FITC-dextrans (10 mg/mL, 2 mL) of two different average M_ws, namely 4400 or 20,400 Da, in HEPES buffer (10 mM, with 100 mM NaCl and 1 mM EDTA sodium, pH 7.4). The size of B3M-liposomes was reduced and made uniform by manual extrusion (8 times through 0.8 μm polycarbonate membranes). A Sepharose™ CL-4B column was used for removal of unentrapped FITC-dextran 4400 and 20,400. HEPES buffer (10 mM, with 100 mM NaCl and 1 mM EDTA sodium, pH 7.4) was used for the elution.

The B3M-liposomes mimicking *P. aeruginosa* membranes were tailored similarly to the *S. aureus* membranes mimics; however, the lipid composition was altered. The membrane was composed of DOPE, DOPG, and cardiolipin (20 mg) in a molar ratio of 65:23:12 as described by Lombardi et al. [36].

2.12.2. FITC-dextran leakage

FITC-dextrans leakage from B3M-liposomes was assessed following the procedures [35,37] with minor modifications. The FITC-dextran-loaded B3M-liposomes were diluted 20-fold in the HEPES buffer. The non-formulated and formulated 7e-SMAMP were also diluted in HEPES buffer (final 7e-SMAMP concentrations corresponding to 0.5, 2, and 5 μg/mL). The leakage from FITC-dextran-loaded B3M-liposomes was measured as a fluorescence intensity at excitation wavelength 485 nm and emission wavelength 530 nm after 10 min. Triton (10 %, *v*/v) in HEPES buffer served as control. The leakage was calculated using the following formula (Eq. (2)) [38]:

$$\text{Leakage } (\%) = 100 \times \left[(F - F_0)/(F_T - F_0)\right] \quad (2)$$

F = fluorescence of treated FITC-dextran B3M-liposomes.F_0 = buffer.F_T = buffer with Triton.

2.12.3. Lipid flip-flop

The B3M-liposomes mimicking *S. aureus* or *P. aeruginosa* membranes for the lipid flip-flop assay were tailored in the same manner as for the FITC-dextran leakage assay; however, C_6-NBD-PG was added at 0.5 mol % together with the other lipids [39]. The lipid film was rehydrated with HEPES buffer (10 mM, comprising 100 mM NaCl and 1 mM EDTA sodium, pH 7.4) and the vesicle size reduced in the same manner as for the FITC leakage assay. To achieve only the labelling of the inner leaflet, sodium dithionite (1 M) in 1 M HEPES buffer (pH 7.4) was added to B3M-liposomes that were incubated for 15 min at 24 °C to ensure quenching of C_6-NBD-PG in the outer leaflets. Subsequently, B3M-liposomes and sodium dithionite were separated on PD-10 desalting columns (Cytiva, Marlborough, MA, USA) with HEPES buffer (10 mM, with 100 mM NaCl and 1 mM EDTA, pH 7.4) sodium for the elution. The B3M-liposomes were diluted 50-fold with buffer and incubated with non-formulated or formulated 7e-SMAMP (0.5, 2, and 5 μg/mL, 7e-SMAMP concentration). Finally, sodium dithionite (1 M) was added, and monitored with excitation and emission wavelengths of 460 and 520 nm, respectively, for 650 s. Triton or buffer served as respective controls [39,40].

2.13. Antimicrobial evaluation

2.13.1. Determination of MIC and MBC

The antimicrobial activity of 7e-SMAMP-liposomes, as well as 7e-SMAMP and empty liposomes, was evaluated by broth microdilution method following the EUCAST guidelines [41]. Microorganisms were aerobically cultured on nutrient agar plates at 37 °C for 24 h, and subsequently diluted in nutrient broth (NB) [26,42] to obtain bacterial suspensions at final concentrations of 2×10^6 CFU/mL. The 7e-SMAMP was solubilized in 100 % dimethyl sulfoxide (DMSO, 10 mg/mL) and then diluted in distilled water to assure that the final concentration of DMSO in the test series was <1 %. The non-formulated and formulated 7e-SMAMP were diluted in sterile water in a two-fold sequence in 96-well culture plates (Corning Inc., Pisa, Italy) to test 7e-SMAMP concentration ranging from 0.1 to 100 μg/mL. Empty liposomes and DMSO were tested at the same dilutions. The microbial suspension (100 μL) was then inoculated with 100 μL of samples. Wells containing microbial suspension (100 μL) and sterile water (100 μL) served as growth control. Blank control, comprising only a growth medium, and sterility controls, containing samples and sterile medium, were also included. Plates were aerobically incubated at 37 °C for 24 h. Afterwards, the minimal inhibiting concentrations (MIC) were determined by comparing the turbidity (OD_{600}) of samples with that of growth control by means of EnSpire Multimode Plate Reader (PerkinElmer Inc., Waltham, MA, USA). To determine a microbicidal effect, 20 μL of samples from wells exhibiting no growth were spotted onto nutrient agar plates and incubated at 37 °C for another 48 h. The minimum bactericidal concentration (MBC) was defined as the minimal concentration that completely inhibited microbial viability. Three batches for each formulation were tested in triplicates.

2.13.2. Killing curves in simulated wound fluid

The antimicrobial activity of non-formulated and formulated 7e-SMAMP was also evaluated against planktonic cultures of pathogens in SWF (bovine serum albumin 2 % *w/v*; $CaCl_2$ 0.02 M; NaCl 0.4 M; Trizma base 0.05 M, pH 7.4) [21]. The 7e-SMAMP was diluted in distilled water starting from the stock solution (10 mg/mL in DMSO) at the same concentration as in liposomes. Both 7e-SMAMP and 7e-SMAMP-liposomes were diluted in 5 mL of SWF to test the final concentration of 50 μg/mL of SMAMP. Empty liposomes were diluted in the same manner. Microorganisms were aerobically cultured on nutrient agar plates at 37 °C for 24 h, and subsequently suspended in SWF to obtain bacterial suspensions at final concentrations of 10^8 CFU/mL. Next, 50 μL of bacterial suspensions were then added to SWF containing free or formulated 7e-SMAMP (starting inoculum of 10^6 CFU/mL). Microorganisms inoculated in 5 mL of SWF were used as controls. Counts of viable cells were carried out on nutrient agar plates at the inoculum time and after 3, 6, 8, and 12 h of incubation at 32 °C. Three batches for each formulation were tested in triplicates. Results are expressed as viability (logCFU/mL) of microorganisms over the time in presence of different samples.

2.13.3. Anti-biofilm activity

The non-formulated and formulated 7e-SMAMP were investigated for their ability to inhibit the biofilm formation and eradicate preformed biofilms of *S. aureus*, *E. coli*, and *P. aeruginosa*. Microbial suspensions were prepared as previously described (2.13.1) and employed as inocula for both the inhibition and eradication assays. For the inhibition assay, the wells of sterile 96-well flat-bottomed culture plates were filled with 100 μL of microbial suspension and 100 μL of non-formulated and formulated 7e-SMAMP. Both non-formulated and formulated 7e-SMAMP were tested at final concentrations of 0.78, 1.56, 3.12, 6.25, 12.5, 25, and 50 μg/mL. The DMSO and empty liposomes were also tested as controls. The multi-well plates were incubated at 37 °C under shaking (100 rpm) for 48 h to allow biofilm development.

For the eradication assay, the 96 multi-well plates were inoculated with 200 μL of bacterial suspensions and after 48 h of incubation (37 °C, 100 rpm), the liquid cultures were removed, leaving only adherent cells. Cells were washed once with phosphate-buffered saline (PBS, pH 7.4), and biofilms were then treated with 100 μL of fresh medium and 100 μL of non-formulated and formulated 7e-SMAMP at the same concentrations as in the inhibition assay. The plates were further incubated (37 °C, 100 rpm) for 24 h.

Biofilm quantification was performed through crystal violet staining. Briefly, the liquid culture was removed, and adherent cells were washed twice with 200 μL of PBS (pH 7.4), fixed with 200 μL of conc. ethanol for 5 min and stained with 180 μL of crystal violet 0.41 % (*w/v*) in 12 % ethanol for 5 min. Excess stain was rinsed out by washing the multi-well plate with PBS thrice. Subsequently, the plates were air dried, the dye bound to the adherent microorganisms was resolubilized with 200 μL of acetic acid 30 % (*v/v*) and the optical density measured at 595 nm (OD_{595}). Three batches for each formulation were tested in triplicates. The anti-biofilm activity was calculated with respect to untreated control, as follows (Eq. (3)):

$$\text{Inhibition of biofilm formation/Eradication of pre-formed biofilm (\%)} = (1\text{-}OD_{595}\ \text{sample}\ /\ OD_{595}\ \text{control}) \times 100 \quad (3)$$

2.14. Statistical analyses

In general, results are expressed as mean ± SD. Student's *t*-tests, one-way ANOVA with Tukey's post-test or two-way ANOVA with Šídák's multiple comparisons post-test were performed to evaluate significance (at least $p < 0.05$). All statistical analyses were performed in GraphPad Prism version 9.3.1 for Windows (GraphPad Software LLC, San Diego, CA, USA).

3. Results and discussions

3.1. 7e-SMAMP stability

AMPs often display instability in different biological fluids; however, this drawback is expected to be addressed by designing SMAMPs. Still, it is important to evaluate the stability of novel SMAMPs as well as their safety prior to the development of pharmaceutical formulations [28].

The chemical stability of 7e-SMAMP was evaluated by analysing the 7e-SMAMP content in fluids after 1- and 7-days storage at 4, 25, and 32 °C. The 7e-SMAMP was stored in either SWF (Fig. 2a) or water (Fig. 2b) and compared to the initial concentrations. As seen in Fig. 2a, the 7e-SMAMP was stable in SWF over the entire period at all temperatures. The stability of the 7e-SMAMP in water (Fig. 2b) was in most cases seemingly lower at 25 and 32 °C; however, the deviations within the same measurements were rather large. Despite more variations upon storage in water, the content remained almost constant throughout the stability testing period. Additionally, the 7e-SMAMP is formulated in delivery systems both to maintain over an extended period at wounded site and be protected against degradation. Furthermore, our results were in agreement with the UV-scans analysis data presented in Supplementary Materials (S2.1.), and indicate that 7e-SMAMP should be stored at 4 °C.

3.2. Liposome characteristics

In the fight against resistant pathogens, new antimicrobial compounds are needed to avoid an even more challenging outcome and further progression of resistance patterns seen today. However, effective means of delivering these active compounds to the targeted site are desired and often necessary to achieve sufficient therapeutic effects. The novel 7e-SMAMP has previously displayed excellent activity against some of the most problematic bacteria; however, its toxicity profile might still limit its applicability in clinical settings [15]. Liposomes are known to reduce the toxicity of pharmaceutical compounds, including

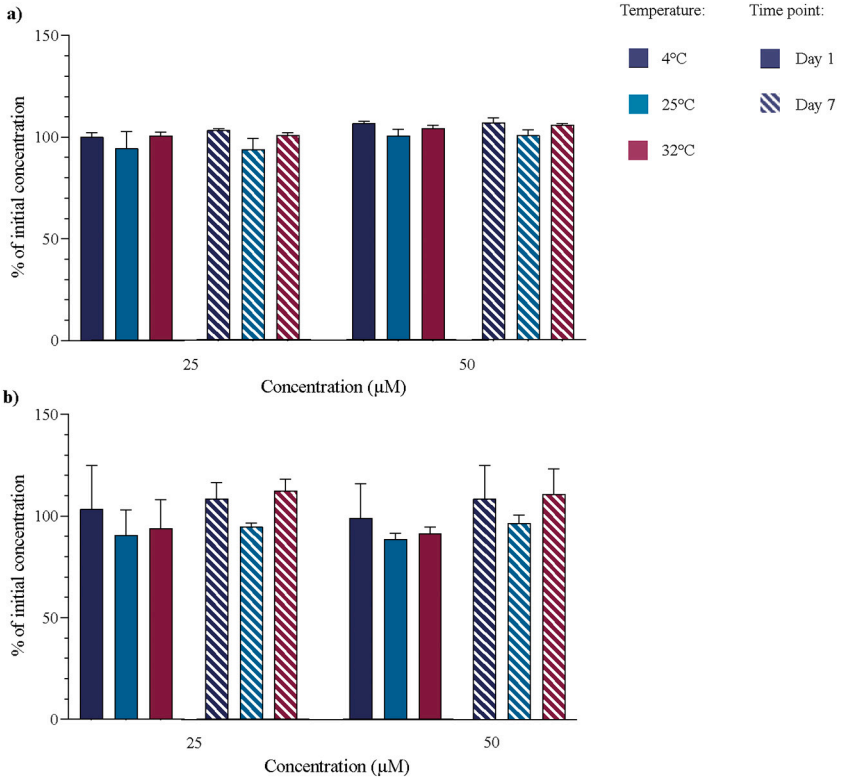

Fig. 2. Stability of non-formulated 7e-SMAMP. The changes from initial concentration (25 and 50 μM) when stored in a) simulated wound fluid (SWF) and b) milli-Q (mQ) water at 4, 25, and 32 °C for 1 day (solid colour) and 7 days (pattern) compared to the determined concentration upon preparation. All results are expressed as means with their respective SD ($n = 3$).

AMPs [23,43]. Moreover, liposomes are known to be able to improve antimicrobial efficacy of antimicrobial compounds both against planktonic and biofilm-embedded bacteria and it has been shown that they interact with skin and can accumulate active compounds at specific sites [44,45]. As exemplified by Rukavina et al., incorporating azithromycin in liposomes significantly lowered both MIC and minimum biofilm inhibitory concentration of azithromycin [46]. Our formulation, comprising liposomes and a SMAMP, could fulfil most crucial requirements; increased activity, reduced toxicity, prolonged release, and maintenance of structural integrity, all required for a successful topical delivery system intended for treatment of infected chronic wounds or other topical infections.

The liposome properties are strongly related to the formulation characteristics and, in the extent of that, the biological properties. In topical delivery, sizes in the range of 200–300 nm are found to be suitable for pharmaceutical delivery vesicles [47,48]. Furthermore, we previously found that liposomes associated with the MAA chlorhexidine, in the same size range, demonstrated promising antimicrobial and antibiofilm activities against *S. aureus* and *P. aeruginosa* [21]. As illustrated in Table 1, the thin film hydration method followed by extrusion, as a size reduction method, resulted in liposomes smaller than 300 nm. Furthermore, these preparation methods also yielded an acceptable polydispersity index (PI) of 7e-SMAMP-liposomes. For lipid-based systems intended for topical delivery, PIs below 0.3 are considered suitable and represent rather homogenous populations [49]. Generally, an overall positive surface charge of vesicles is preferred when tailoring drug delivery systems for microbial and biofilm eradication [43,50]. The bacterial membrane is negatively charged, therefore liposomes with a positive surface charge can easily interact with the membrane. A strengthened electrostatic interaction between the bacterial membrane and liposomes could result in a successful outcome [51]. This interaction is potentially stronger with bacterial compared to eukaryotic membranes due to the slightly higher negative charge density on bacterial membranes [52]. This may lead to reduced toxicity and a favourable outcome of treatment with the novel SMAMP; however, the biocompatibility needs to be assessed. Literature also shows that cationic liposomes might improve inhibition of biofilm formation [44]. The high zeta potential of 7e-SMAMP-liposomes (58.7 mV) could most likely be ascribed to 7e-SMAMP association with/in bilayers of liposomes. This indicated that the cationic guanidine groups of 7e-SMAMP (Fig. 1) are accommodated onto/within the lipid bilayer This association also resulted in a rather high entrapment efficiency of 78 %, as seen in Table 1.

Considering wound healing, acidic pH conditions could be advantageous. The most common bacteria have optimal growth at neutral pH conditions, therefore lowered pH could generate less favourable conditions for the bacterial growth [53]. Although this alone is not enough to prevent bacterial growth, acidic pH of 7e-SMAMP is highly beneficial feature considering therapy.

In the quality control of liposomes or other lipid-based formulations, it is important to monitor the lipid content of formulations, especially when reducing the size of liposomes by extrusion. The phospholipid content of 7e-SMAMP-liposomes was approximately 90 % (Table 2),

Table 1
Liposome characteristics: mean diameter, polydispersity index (PI), zeta potential, entrapment efficacy (EE%), and pH in aqueous medium.

	Mean diameter (nm)	PI	Zeta potential (mV)	EE (%)	pH
7e-SMAMP-liposomes	276 ± 16	0.20 ± 0.01	58.7 ± 1.6	78.1 ± 2.2	4.9 ± 0.1
Empty liposomes	269 ± 42	0.44 ± 0.05	−0.4 ± 0.2	–	6.3 ± 0.0

Results are expressed as means with their respective SD ($n = 3$). The mean diameter represents the weight-intensity distribution of the liposomes.

Table 2
Phospholipid content and membrane elasticity of liposomes.

	Phospholipid content (%)[a]	Membrane elasticity (E)
7e-SMAMP-liposomes	89.9 ± 1.0	5.081 ± 0.785
Empty liposomes	92.6 ± 1.7	9.775 ± 0.581

Results are expressed as means with their respective SD (n = 3).
[a] Phospholipid content (%) of initial concentration (20 mg/mL).

proving limited loss of lipid during the extrusion process. To further examine the stability of liposomes after incorporation of 7e-SMAMP, the membrane elasticity assay was performed. AMPs and SMAMPs are reported to destabilize the bacterial membrane [54]; we therefore sought to investigate if the membrane integrity of liposomes was altered by 7e-SMAMP. As seen in Table 2, the rigidity of the bilayer of 7e-SMAMP-liposomes was higher ($p = 0.001$) than for the empty liposomes, indicating that the bilayer of the 7e-SMAMP-lipsomes remained stable upon incorporation of 7e-SMAMP. A small increase in fluidity could be linked to the so-called carpet-like model of their antimicrobial mechanisms of action; a contribution because of disruption of lipid packing within the membrane [55]. Furthermore, the 7e-SMAMP-liposomes maintained a stable size, size distribution, surface charge, entrapment efficacy, and pH over a period of 12 weeks (Table S1).

Since liposomes incorporating 7e-SMAMP were prepared for the first time, we utilized TEM to evaluate the morphology and confirm the size of the novel 7e-SMAMP-liposomes. The 7e-SMAMP-liposomes were spherical and in similar size range as determined using dynamic light scattering (Fig. 3a). Additionally, TEM was also used to confirm the formation of liposomes and their structure, even upon incorporation of 7e-SMAMP. Fig. 3b demonstrates the proposed accommodation of 7e-SMAMP within the liposomal bilayers.

3.3. In vitro release

The conventional formulations for localized antimicrobial therapy of the skin, especially considering wounds, are often associated with serious limitations such as instability of drug at the site of application and/or insufficient drug release leading to low drug concentration at the site of infection [46]. Therefore, the first aim was to tailor a formulation able to remain at the intended site and serves as a depot of the antimicrobial compound assuring its prolonged release. Secondly, the formulation should ensure proper release of the antimicrobial compound to achieve a high local concentration to prevent bacterial growth, eradicate existing bacteria and inhibit biofilm formation or eliminate biofilm-embedded bacteria [56]. As shown in Fig. 4 the release from the 7e-SMAMP-liposomes was approximately 71 % (after 8 h) and 79 % (after 24 h), respectively, while for the free or non-formulated 7e-SMAMP, 94 % of the content permeated through the membrane after only 6 h. The release from liposomes was significantly slowed ($p <$

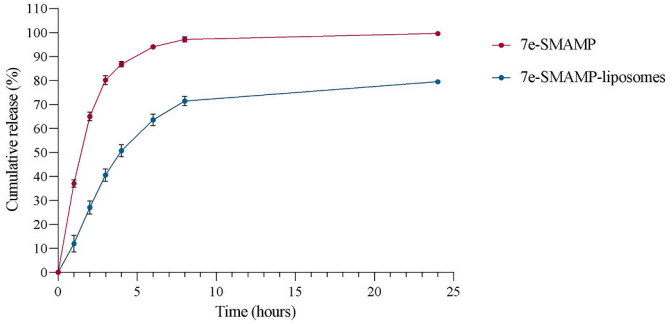

Fig. 4. Cumulative release (%) from non-formulated (dissolved in release medium, free) and formulated 7e-SMAMP utilizing dialysis membranes (32 °C, 24 h). The release is presented as the cumulative percentage of the initial liposomally-associated 7e-SMAMP concentration. All results are expressed as means with their respective SD ($n = 3$).

0.0001 for all time points) as compared to non-formulated 7e-SMAMP (free). Therefore, this rather high initial concentration could boost the immediate eradication, while slower release after 6–8 h could prevent bacterial regrowth. Furthermore, liposomes could interact with the bacterial membrane and give increased concentration of the antimicrobial compound within bacteria [57].

Reducing the frequency of formulation application onto an already painful area is considered beneficial in the treatment of chronic wounds [21]. The 7e-SMAMP-liposomes decreased the release rate of 7e-SMAMP and could potentially allow for less frequent administration onto wounded areas. Furthermore, according to Korrapati and colleagues, ideal biological nanomaterials should be easy to design and modify, originate from natural sources and be biodegradable, biocompatible, and non-toxic [58]. Liposomes possess all these features; namely, are made of lipids originating from natural sources are biodegradable, non-toxic, and biocompatible, especially considering skin and the moist environment in wounds [59]. However, liposomal formulations do not exhibit proper viscosity as well as desired retention and are often incorporated within secondary delivery system (vehicle), such as hydrogels, that can be tailored to improve the healing while treating infection intended for wounds [21].

3.4. Evaluation of cell viability

Biocompatibility of drug formulation is an important issue, especially considering its contact with the wound [3]. Since 7e-SMAMP requires a smart formulation to be administered, the potential cytotoxicity of 7e-SMAMP-liposomes in comparison to empty liposomes was investigated *in vitro* using murine macrophages and keratinocytes. In both cell lines, the cell viability for liposomes-treated cells was similar to the non-treated cells (Fig. 5a). However, both macrophages and keratinocytes

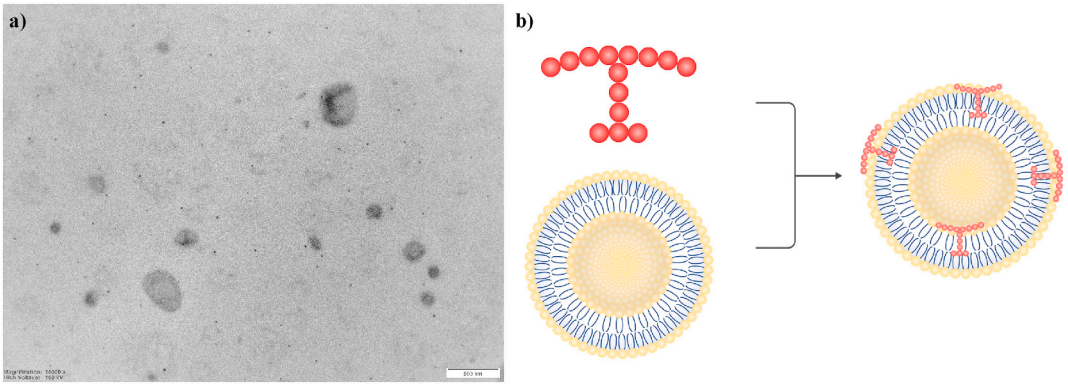

Fig. 3. a) TEM image of 7e-SMAMP-liposomes. Scale bar 500 nm. b) Proposed accommodation of 7e-SMAMP in liposomes.

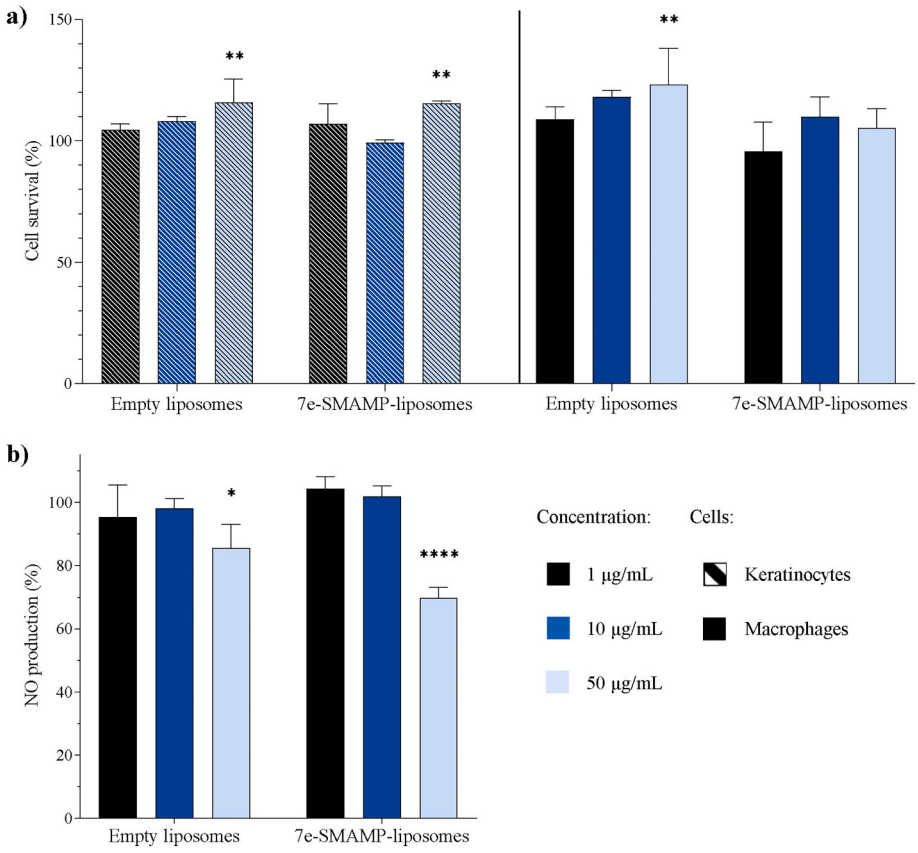

Fig. 5. a) Evaluation of cell toxicity of empty and 7e-SMAMP-liposomes in HaCaT (patterned bars, left) and RAW 264.7 cells (solid bars, right). Three different concentrations were tested, namely 1, 10, and 50 µg/mL lipid, and the results are presented as cell viability of treated cells compared to control (100 %). Control cells were only supplemented with complete medium; the cell viability is thereof considered as 100 %. b) Evaluation of anti-inflammatory activity of empty liposomes and 7e-SMAMP-liposomes expressed as reduction of nitric oxide (NO) production in RAW 264.7 cells. Three different concentrations were tested, namely 1, 10, and 50 µg/mL lipid, and the results are presented as NO production of treated cells compared to control (100 %). Control refers to non-treated lipopolysaccharide (LPS)-induced cells; their production is thereof considered as 100 %. All results are expressed as means with their respective SD ($n = 3$). * $p \leq 0.05$, ** $p \leq 0.01$, **** $p \leq 0.0001$, compared to control.

treated with the highest concentration (50 µg/mL) of empty liposomes demonstrated significantly improved viability ($p < 0.01$), while keratinocyte viability improved at the highest concentration of 7e-SMAMP-liposomes ($p < 0.01$). Highly cationic surfaces of liposomes, as in our case, could alter the safety profile of the formulation [60]. Nevertheless, no negative effects of empty or 7e-SMAMP-liposomes were observed in the current study. The dose-dependent cell compatibility and proliferative effects of empty liposomes have previously been confirmed in both macrophages and keratinocytes [33,61].

3.5. Anti-inflammatory activity

The wound healing cascade is both dynamic and complex, and therefore depends on several intricately tuned events to transpire [62]. In this cascade, macrophages are essential for removal of debris, damaged matrix, microorganisms, and neutrophils from the wound bed in addition to releasing cytokines and growth factors [63]. Throughout wound healing process, pro-inflammatory macrophages transition into an anti-inflammatory macrophage phenotype to initiate healing [64]. However, in chronic wounds, transition to the next stages is hampered and the wound becomes haltered in the inflammatory phase [65]. Furthermore, many chronic wounds exhibit higher levels of NO that could cause damages to the tissue in the later stages of the cascade [66]. Therefore, we evaluate the anti-inflammatory activity of both empty and 7e-SMAMP-liposomes through their ability to lower inflammatory response by reducing the NO production in LPS-induced murine macrophages as an indicator for the liposomes' anti-inflammatory potential. As shown in Fig. 5b, the highest lipid concentration of both empty and 7e-SMAMP-liposomes significantly ($p < 0.05$ and $p < 0.0001$, respectively) reduced the NO production compared to the non-treated cells (control cells).

In the current study, we observed a clear indication of the dose-dependent anti-inflammatory trends when 7e-SMAMP was incorporated within liposomes. The findings are in agreement with the work by Ahn et al. who investigated the anti-inflammatory properties of a peptidomimetic in the same cell line as used in our work; the authors also found a dose-dependent reduction in inflammatory response upon treatment with the peptidomimetic [67]. Moreover, we also detected anti-inflammatory activity of empty liposomes, similarly as Giordani et al. who reported reduced NO production in LPS-induced macrophages by approximately 20 % compared to the non-treated cells evaluated in the same concentration range [68].

3.6. Effect of formulated and non-formulated 7e-SMAMP on bacterial membrane-mimic liposome models

Liposomes tailored to mimic bacterial membranes are often utilized to investigate the potential antimicrobial and membrane-activity of MAAs, also termed transient pore formation [36,69]. We assessed the activity of both non-formulated and formulated 7e-SMAMP on B3M-liposomes mimicking *S. aureus* and *P. aeruginosa* membranes by studying the leakage of liposomally-associated FITC-4400 or FITC-20400, respectively. As shown in Fig. 6, both non-formulated and formulated 7e-SMAMP induced leakage from mimicked *S. aureus* (Fig. 6a and b) and *P. aeruginosa* (Fig. 6c and d) B3M-liposomes. A dose-dependent leakage was observed; however, it was more pronounced in the mimicked *S. aureus* B3M-liposomes. Stronger antimicrobial activity against gram-positive strains is commonly observed for both AMPs and SMAMPs due to their membrane structure [15,70]. In our study, the leakage was stronger for non-formulated 7e-SMAMP than formulated 7e-SMAMP, while FITC-4400 leakage was slightly higher than FITC-20400 leakage, as expected due to smaller M_w. In mimicked *P. aeruginosa* B3M-liposomes, the dose-dependency was not as evident for non-formulated 7e-SMAMP; however, the differences in leakage between the two markers were observed. Leakage of FITC-4400 was greater when the B3M-liposomes were treated with non-formulated 7e-SMAMP; in

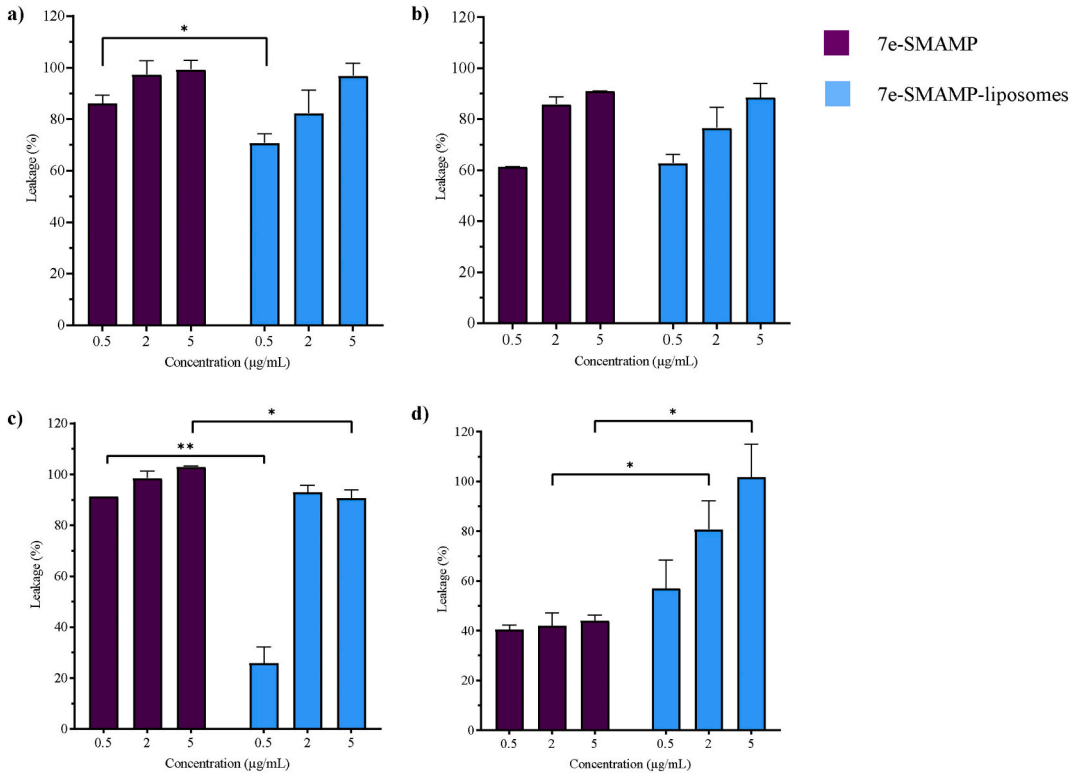

Fig. 6. Bacterial Membrane-Mimic Liposomes Models (B3M-liposomes) loaded with FITC-dextran 4400 or 20,400 (molecular weight = M_w) treated with 7e-SMAMP or 7e-SMAMP-liposomes. The leakage is expressed as percentage compared to the control (Triton X-100). Concentrations of 7e-SMAMP were 0.5, 2, and 5 µg/mL for both non-formulated and formulated 7e-SMAMP. Different B3M-liposome mimics were prepared and challenged, namely A) *S. aureus* with FITC-4400, B) *S. aureus* with FITC-20400, C) *P. aeruginosa* with FITC-4400, and D) *P. aeruginosa* with FITC-20400. Results are presented as means with their respective SD ($n = 3$). *) $p < 0.05$, **) $p < 0.01$.

addition, a clear dose/effect step was observed between 0.5 and 2 µg/mL upon treatment with formulated 7e-SMAMP. Leakage of FITC-20400 was only about 40 % and approximately the same for all concentrations of non-formulated 7e-SMAMP. The mimicked *P. aeruginosa* B3M-liposomes loaded with FITC-20400 treated with formulated 7e-SMAMP displayed much greater leakage in a dose-dependent manner. Other studies have also confirmed dose-dependent leakage from membrane-mimics, as in the study of Lee et al. where they assessed calcein leakage from *Escherichia coli* mimics [69]. Furthermore, Lombardi et al. showed dose-dependent leakage of 8-aminonaphtalene-1,3,6-trisulfonic acid disodium salt in membrane-mimics of *E. coli* and *P. aeruginosa* [36].

Another approach to investigate the membrane-activity of MAAs is to examine the fusion between the inner and outer layer of mimicked B3M-liposomes. Here, the B3M-liposomes were labelled only on the inner leaflet by reducing the labelling on the outer layer using a reducing agent [36]. In the mimicked *S. aureus* B3M-liposomes (Fig. 7a), the initial leaflet fusion of mimics treated with non-formulated 7e-SMAMP showed dose-dependent trends. Mimicked *S. aureus* B3M-liposomes treated with formulated 7e-SMAMP showed different tendencies. At the highest 7e-SMAMP concentrations, the fusion was quite extensive and exhibited an initially stronger effect than the control (Triton); however, the leaflet fusion gradually turned similar for different concentrations. In the mimicked *P. aeruginosa* B3M-liposomes (Fig. 7b), Triton exhibited the strongest fusion activity overall. Additionally, both the non-formulated and formulated 7e-SMAMP demonstrated dose-dependent lipid flip-flop activity. Yet, the formulated 7e-SMAMP seemingly had a stronger effect on the inner-outer leaflet fusion than the non-formulated 7e-SMAMP indicating higher stress responses on the membranes. This was in line with the results from the evaluation of FITC leakage from B3M-liposomes. Strong effects on inner-leaflet-labelled

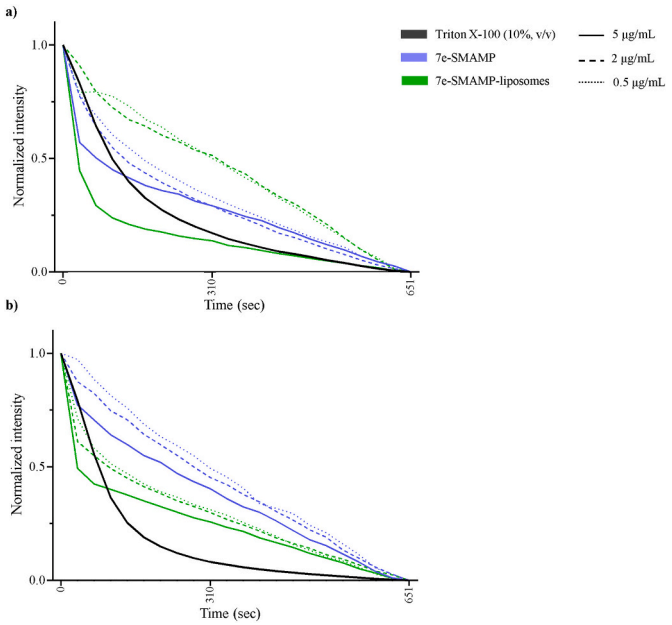

Fig. 7. Lipid flip-flop in Bacterial Membrane-Mimic Liposomes Models (B3M-liposomes) of bacterial membranes with C6-NBD-PG inner leaflet labelling. The B3M-liposomes were treated with non-formulated and formulated 7e-SMAMP and monitored for 650 s. Two different B3M-liposome mimics were prepared and challenged, namely A) *S. aureus* and B) *P. aeruginosa* B3M-liposome mimics. Concentrations of 7e-SMAMP were 0.5, 2, and 5 µg/mL were chosen for both non-formulated and formulated 7e-SMAMP. Results are presented as means of the normalized fluorescence intensity (0–1, $n = 3$).

liposomes have previously been showed in other studies [71]. Additionally, dose-dependent responses have also earlier been confirmed for AMPs [39,72].

3.7. Antimicrobial activity

3.7.1. Inhibitory activity towards planktonic cultures

Antimicrobial wound management is a major challenge that highlights the need for new solutions against free-floating pathogens and their biofilms. After a first contamination, the wound microenvironment can be rapidly colonized by gram-positive bacteria, specifically *S. aureus*, followed by gram-negative bacteria, including *P. aeruginosa* and *E. coli*. During acute wound infections, local therapy is highly beneficial to immediately inhibit microbial proliferation, and therefore, prevent the spread and chronification of wounds. Unfortunately, the tendency of microorganisms such as *S. aureus* to easily acquire MDR makes most of the conventional available therapies ineffective [73,74]. In this regard, AMPs and SMAMPs are intriguing alternatives to counteract bacterial spreading. Paulsen et al. have already reported that free 7e-SMAMP possesses promising antibacterial activity both *in vitro* and in a murine model [15]. Considering that delivery system is expected to enhance the activity on incorporated antimicrobial [21], we developed novel 7e-SMAMP liposomes and, tested their antimicrobial activity against planktonic cultures of susceptible bacteria (*S. aureus* ATCC29213, *E. coli* ATCC11105, and *P. aeruginosa* ATCC10145), gentamicin-resistant *S. aureus* (SO88) and MDR *S. aureus* (SO2, SO83, and SO86). The MIC and MBC values are reported in Table 3. Empty liposomes and DMSO did not affect the bacterial growth, as expected (data not shown). We were concern whether liposomal incorporation can hamper the activity of 7e-SMAMP. The 7e-SMAMP-liposomes exhibited the same MIC and MBC values as non-formulated 7e-SMAMP, indicating that neither the delivery system nor the preparation procedure interfered with the biological activity of the payload.

Among tested bacteria, inhibiting *P. aeruginosa* ATCC10145 was the most challenging (MIC: 25.00 μg/mL), whilst *S. aureus* ATCC29213 and *S. aureus* SO88 were very sensitive to the action of 7e-SMAMP-liposomes (MIC: 0.78–1.56 μg/mL). Notably, 7e-SMAMP-liposomes were also effective against MDR *S. aureus*, although MIC values (MIC: 3.13–12.50 μg/mL) were higher than those obtained for the susceptible strain. Overall, the MBC values were only slightly higher than MIC values suggesting that 7e-SMAMP acted as bactericidal compound. This was in full agreement with Paulsen et al. who previously demonstrated that 7e-SMAMP possesses membranolytic dose-dependent activity against both gram-positive and gram-negative bacteria [15].

To mimic the microenvironment at the wound site, the viability of *S. aureus, E. coli*, and *P. aeruginosa* was assessed in SWF [75] and compared with that of the same bacteria in the presence of non-formulated and formulated 7e-SMAMP (Fig. 8). The 7e-SMAMP concentration was adjusted to 50 μg/mL because it was proven to be bactericidal for all tested microorganisms (Table 3). In the control, cell viability was retained over time, as well as in the presence of empty liposomes. Considering susceptible bacteria, 7e-SMAMP showed high potency against *S. aureus* ATCC29213 and a slightly lower activity against *E. coli* ATCC11105 and *P. aeruginosa* ATCC10145. Indeed, after 3 h of incubation, *S. aureus* ATCC29213, *E. coli* ATCC11105, and *P. aeruginosa* ATCC10145 viability was reduced by 3.84, 2.90, and 2.38 logCFU/mL, respectively. This suggested that gram-positive bacteria were more efficiently killed than gram-negative bacteria, possibly because the outer membrane of the latter hindered 7e-SMAMP bacteriolytic effect. Importantly, drug resistant *S. aureus* strains were only slightly more difficult to inhibit compared to sensitive *S. aureus* ATCC29213. Indeed, the viability of *S. aureus* SO2, SO83, SO86, and SO88 decreased by 2.28–2.96 logCFU/mL after 3 h of incubation and was completely abolished after 12 h as for sensitive pathogens. An almost complete killing effect was also detected for 7e-SMAMP-liposomes within 12 h, but with a delayed action, in agreement with the release profile of 7e-SMAMP (Section 3.3.). However, already after 8 h of treatment the bacterial load was reduced by at least 3 logCFU/mL, except for *S. aureus* SO2, indicating that concentration of 7e-SMAMP released in this time-window was enough to elicit a first strong antimicrobial activity. After 12 h, the inhibition of bacterial growth was even more pronounced, with complete killing of all bacterial strains, except from *S. aureus* SO2 and *P. aeruginosa* ATCC10145. However, the viability of these strains was reduced by at least 4.99 logCFU/mL, thus confirming that the liposome formulation was able to assure a prolonged 7e-SMAMP action.

Table 3
Antimicrobial activity (MIC and MBC) of non-formulated and formulated 7e-SMAMP.

	MIC (μg/mL)		MBC (μg/mL)	
	7e-SMAMP	7e-SMAMP-liposomes	7e-SMAMP	7e-SMAMP-liposomes
S. aureus ATCC29213	0.78	0.78	3.13	3.13
S. aureus SO2	12.50	12.50	25.00	25.00
S. aureus SO83	6.25	6.25	12.50	12.50
S. aureus SO86	3.13	3.13	6.25	6.25
S. aureus SO88	1.56	1.56	6.25	6.25
E. coli ATCC11105	3.13	3.13	6.25	6.25
P. aeruginosa ATCC10145	25.00	25.00	50.00	50.00

MIC: minimal inhibitory concentration; MBC: minimum bactericidal concentration (n = 3).

3.7.2. Activity towards biofilms

The formation of biofilms at the infection site can delay/hamper the healing process, which in turn leads to chronic infections [74]. It has been proposed that AMPs and SMAMPs are promising as anti-biofilm compounds as compared to conventional antibiotics since their bactericidal and/or bacteriostatic activities primarily depend on their ability to interact with bacterial membranes or cell walls, regardless of the bacterial metabolic state [54,76]. Results reported in Section 3.6. proved that 7e-SMAMPs, as well as 7e-SMAMPs-liposomes, can interact with *S. aureus* and *P. aeruginosa* membranes. Thus, we also investigated the potential of non-formulated and formulated 7e-SMAMP to inhibit biofilm formation (Fig. 9) and eradicate pre-formed biofilms (Fig. 10). Generally, bacterial biofilms exhibit higher resistance to antimicrobials compared to planktonic bacteria, due to difficulty of penetrating capsular polysaccharides [77]. Non-formulated 7e-SMAMP completely inhibited *S. aureus* ATCC29213 biofilm formation at 6.25 μg/mL (Fig. 9), and eradicated pre-formed biofilms at 12.5 μg/mL (Fig. 9), confirming the promising effect of 7e-SMAMP against this strain. Consistent with what has been previously observed for planktonic cultures (Fig. 8), the biofilm of *S. aureus* ATCC29213 was the most sensitive to 7e-SMAMP.

The non-formulated 7e-SMAMP exerted anti-biofilm activity even towards MDR *S. aureus* strains (SO2, SO83, and SO86). However, concentrations above MIC values were required and their eradication was more challenging than the sensitive *S. aureus* ATCC29213. The same trends were observed for gentamicin-resistant *S. aureus* SO88, *E. coli*, and *P. aeruginosa*. Even though, inhibition of biofilm formation in *P. aeruginosa* reached only 86 % at 7e-SMAMP concentration of 50 μg/mL.

As demonstrated in Figs. 9 and 10, association of 7e-SMAMP within bilayers of phosphatidylcholine liposomes significantly improved its anti-biofilm activity, particularly against *S. aureus* SO88 and ATCC29213 biofilms, thus preventing the biofilm formation even at the SMAMP concentrations close to MIC values (Fig. 9). Similar patterns were also confirmed for eradication ability of 7e-SMAMP-liposomes towards pre-formed bacterial biofilms (Fig. 10), although the effective 7e-SMAMP concentrations were significantly higher than for biofilm inhibition (Fig. 9). In MDR strains, the 7e-SMAMP-liposomes

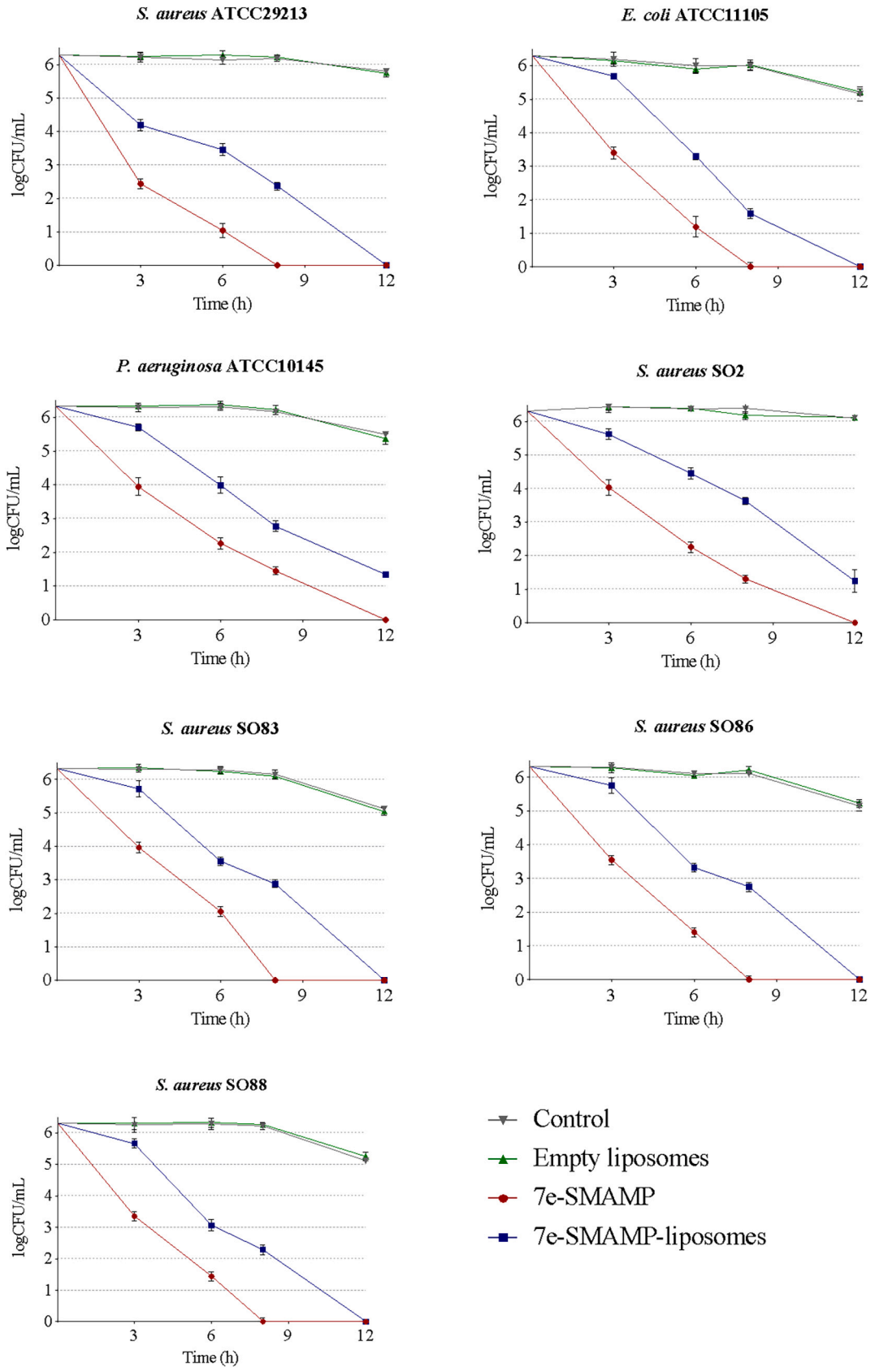

Fig. 8. Viability (logCFU/mL) of bacteria over the time in simulated wound fluid (up to 12 h) in the presence of non-formulated and formulated 7e-SMAMP. The results are presented as the mean of three replicates with their respective SD.

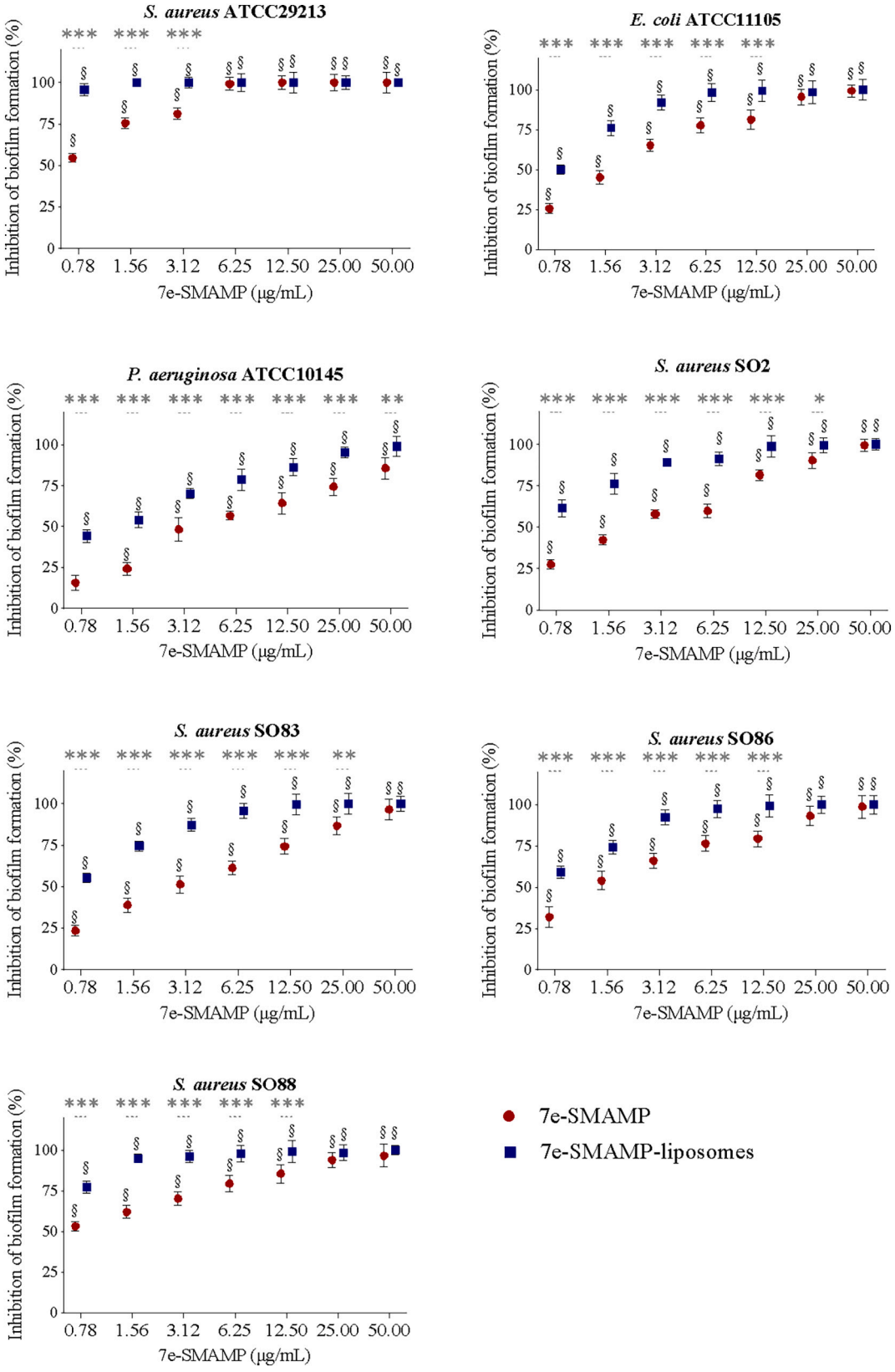

Fig. 9. Anti-biofilm activity: inhibition of the biofilm development (%). The results are presented as the mean of three replicates with their respective SD. §: $p < 0.05$ compared to control. Significant differences between non-formulated and formulated 7e-SMAMP were also reported: *** $p < 0.001$, ** $p < 0.005$.

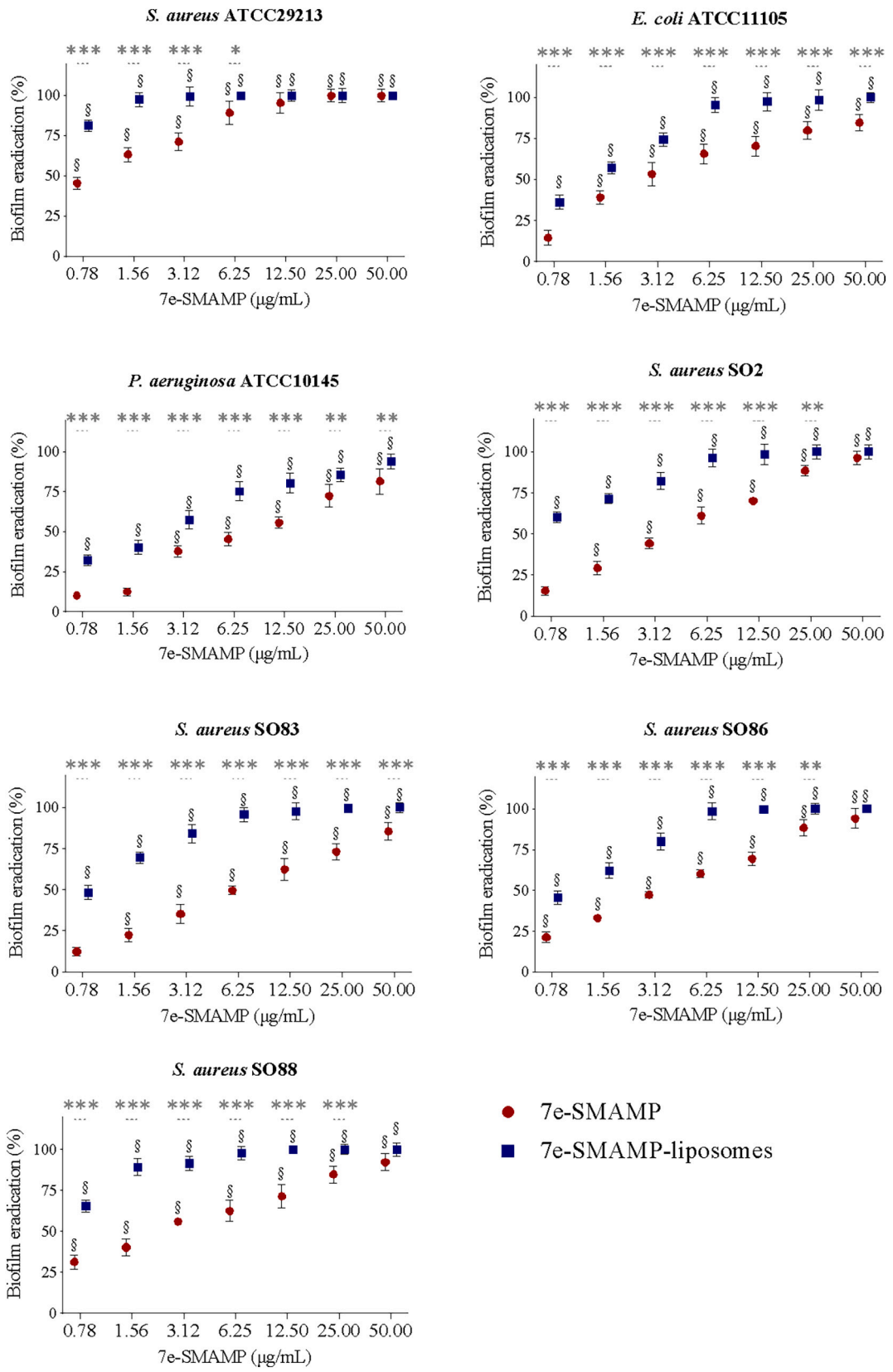

Fig. 10. Anti-biofilm activity: eradication of pre-formed biofilm (%). The results are presented as the mean of three replicates with their respective SD. §: $p < 0.05$ compared to control. Significant differences between non-formulated and formulated 7e-SMAMP were also reported: *** $p < 0.001$, ** $p < 0.005$, * $p < 0.01$.

(formulated) were able to inhibit biofilm formation and eradicate pre-formed biofilms at concentrations close to MIC values, however, slightly higher concentrations were required for *S. aureus* SO86. We confirmed the superiority of formulated 7e-SMAMP's as compared to non-formulated 7e-SMAMP. The inhibition and eradication of gram-negative bacterial biofilms were more challenging than for the gram-positive bacteria, especially for *P. aeruginosa* ATCC10145. In *E. coli* ATCC11105, biofilm inhibition and eradication required concentrations above MIC values (6.25 μg/mL, Figs. 9 and 10). The most challenging bacteria, *P. aeruginosa* ATCC10145, required even higher concentrations for the same activity, in line with the higher MIC values (Table 3).

Many relevant medical pathogens, including *S. aureus*, *E. coli*, and *P. aeruginosa*, comprise negatively charged biofilm extracellular matrix due to the presence of anionic exopolysaccharide and extracellular DNA [78,79]. In this regard, the incorporation of 7e-SMAMP inside liposomes resulted in positive surface charge (Table 1), which can aid the penetration into the extracellular matrix of the biofilm, thus increasing the anti-biofilm capability of the payload [50]. Conventional liposomes have been shown to successfully improve cellular uptake [80]. Moreover, liposomes prepared with the phosphatidylcholine revealed optimal ability to enhance the anti-biofilm activity of chlorhexidine [21]. Here, we confirmed that phosphatidylcholine liposomes were effectively suitable as nanocarrier to target pathogens' biofilms. Indeed, 7e-SMAMP exerted a significantly more efficient anti-biofilm activity when delivered in liposomes than when applied in its non-formulated form. In particular, the capability to eradicate pre-formed biofilms was greatly improved as demonstrated by the complete eradication of biofilms for 7e-SMAMP-liposomes concentrations above 6.25 μg/mL, with the only exception for *P. aeruginosa* ATCC10145. However, even this biofilm was reduced by 75 % when treated with 6.25 μg/mL 7e-SMAMP-liposomes, compared to 45 % eradication in the presence of non-formulated 7e-SMAMP at the same concentration. Moreover, 7e-SMAMP-liposomes strongly hampered pathogens' biofilm formation, with inhibition efficacy close to 100 %, for concentrations at least equal to MIC, especially for gram-positive strains. At the lower tested concentrations, 7e-SMAMP-liposomes were always more efficient in inhibiting the development of biofilms than non-formulated 7e-SMAMP ($p < 0.05$). Taken together these results suggest that 7e-SMAMP-liposomes can be employed both for the prevention of the onset of severe infections and treatment of chronic wound infections.

4. Conclusions

In order to address the limitations and improve the antimicrobial potential of AMPs and SMAMPs, a novel antimicrobial, 7e-SMAMP, was incorporated in liposomes destined for the treatment of biofilm-infected chronic wounds. The 7e-SMAMP-liposomes were evaluated for their *in vitro* biological and antimicrobial activities. The newly developed formulation displayed superior *in vitro* anti-inflammatory responses and had no negative effect on the cellular viability as confirmed in macrophages and keratinocytes. Additionally, the anti-biofilm activities of 7e-SMAMP liposomes against *S. aureus*, *E. coli*, and *P. aeruginosa* were improved as compared to the non-formulated 7e-SMAMP. These superior anti-biofilm effects were proven in both biofilm formation and eradication of pre-formed biofilms. The results supported our hypothesis that 7e-SMAMP-liposomes could serve as a novel platform in the development of antimicrobial therapeutic options for the treatment of biofilm-infected chronic wounds.

Funding sources

The study was funded by UiT The Arctic University of Norway, Norway (project no. 235569). The publication fund of UiT The Arctic University of Norway covered the publication charges of this article.

CRediT authorship contribution statement

Lisa Myrseth Hemmingsen: Conceptualization, Data curation, Formal analysis, Investigation, Methodology, Visualization, Validation, Writing – original draft, Writing – review & editing. **Barbara Giordani:** Data curation, Formal analysis, Investigation, Methodology, Validation, Writing – original draft, Writing – review & editing. **Marianne H. Paulsen:** Writing – review & editing. **Željka Vanić:** Data curation, Formal analysis, Investigation, Methodology, Writing – review & editing. **Gøril Eide Flaten:** Conceptualization, Writing – review & editing. **Beatrice Vitali:** Methodology, Validation, Resources, Writing – review & editing. **Purusotam Basnet:** Methodology, Validation, Writing – review & editing. **Annette Bayer:** Conceptualization, Writing – review & editing. **Morten B. Strøm:** Conceptualization, Funding acquisition, Project administration, Writing – review & editing. **Nataša Škalko-Basnet:** Conceptualization, Funding acquisition, Methodology, Resources, Supervision, Writing – original draft, Writing – review & editing.

Declaration of competing interest

The authors declare the following financial interests/personal relationships which may be considered as potential competing interests:

Marianne H. Paulsen has patent #WO/2018/178198 issued to UiT The Arctic University of Norway. Annette Bayer has patent #WO/2018/178198 issued to UiT The Arctic University of Norway. Morten B. Strom has patent #WO/2018/178198 issued to UiT The Arctic University of Norway.

Data availability

Data will be made available on request.

Acknowledgements

The authors would also like to thank Manuel K. Langer at Department of Chemistry, UiT The Arctic University of Norway for assistance in SMAMP synthesis and Randi Olsen at The Advanced Microscopy Core Facility, Department of Medical Biology, UiT The Arctic University of Norway for the assistance in TEM-imaging The graphical abstract and figures were created with BioRender.com.

Appendix A. Supplementary data

Supplementary data to this article can be found online at https://doi.org/10.1016/j.bioadv.2022.213238.

References

[1] C.J.L. Murray, K.S. Ikuta, F. Sharara, L. Swetschinski, G. Robles Aguilar, A. Gray, C. Han, C. Bisignano, P. Rao, E. Wool, et al., Global burden of bacterial antimicrobial resistance in 2019: a systematic analysis, Lancet 399 (2022) 629–655, https://doi.org/10.1016/S0140-6736(21)02724-0.

[2] P. Beyer, S. Paulin, The antibacterial research and development pipeline needs urgent solutions, ACS Infect. Dis. 6 (2020) 1289–1291, https://doi.org/10.1021/acsinfecdis.0c00044.

[3] B. Blanco-Fernandez, O. Castaño, M.Á. Mateos-Timoneda, E. Engel, S. Pérez-Amodio, Nanotechnology approaches in chronic wound healing, Adv. Wound Care 10 (2020) 234–256, https://doi.org/10.1089/wound.2019.1094.

[4] M. Malone, T. Bjarnsholt, A.J. McBain, G.A. James, P. Stoodley, D. Leaper, M. Tachi, G. Schultz, T. Swanson, R.D. Wolcott, The prevalence of biofilms in chronic wounds: a systematic review and meta-analysis of published data, J. Wound Care 26 (2017) 20–25, https://doi.org/10.12968/jowc.2017.26.1.20.

[5] S. Darvishi, S. Tavakoli, M. Kharaziha, H.H. Girault, C.F. Kaminski, I. Mela, Advances in the sensing and treatment of wound biofilms, Angew. Chem. Int. Ed. 61 (2022), e202112218, https://doi.org/10.1002/anie.202112218.

[6] X. Song, P. Liu, X. Liu, Y. Wang, H. Wei, J. Zhang, L. Yu, X. Yan, Z. He, Dealing with MDR bacteria and biofilm in the post-antibiotic era: application of antimicrobial peptides-based nano-formulation, Mater. Sci. Eng. C 128 (2021), 112318, https://doi.org/10.1016/j.msec.2021.112318.

[7] L. Boge, K. Hallstensson, L. Ringstad, J. Johansson, T. Andersson, M. Davoudi, P. T. Larsson, M. Mahlapuu, J. Håkansson, M. Andersson, Cubosomes for topical delivery of the antimicrobial peptide LL-37, Eur. J. Pharm. Biopharm. 134 (2019) 60–67, https://doi.org/10.1016/j.ejpb.2018.11.009.

[8] S. Singh, A. Numan, H.H. Somaily, B. Gorain, S. Ranjan, K. Rilla, H.R. Siddique, P. Kesharwani, Nano-enabled strategies to combat methicillin-resistant Staphylococcus aureus, Mater. Sci. Eng. C 129 (2021), 112384, https://doi.org/10.1016/j.msec.2021.112384.

[9] C.D. Fjell, J.A. Hiss, R.E.W. Hancock, G. Schneider, Designing antimicrobial peptides: form follows function, Nat. Rev. Drug Discov. 11 (2012) 37–51, https://doi.org/10.1038/nrd3591.

[10] A.T.Y. Yeung, S.L. Gellatly, R.E.W. Hancock, Multifunctional cationic host defence peptides and their clinical applications, Cell. Mol. Life Sci. 68 (2011) 2161–2176, https://doi.org/10.1007/s00018-011-0710-x.

[11] C. Ghosh, P. Sarkar, R. Issa, J. Haldar, Alternatives to conventional antibiotics in the era of antimicrobial resistance, Trends Microbiol. 27 (2019) 323–338, https://doi.org/10.1016/j.tim.2018.12.010.

[12] D. Ciumac, H. Gong, X. Hu, J.R. Lu, Membrane targeting cationic antimicrobial peptides, J. Colloid Interface Sci. 537 (2019) 163–185, https://doi.org/10.1016/j.jcis.2018.10.103.

[13] U. Piotrowska, M. Sobczak, E. Oledzka, Current state of a dual behaviour of antimicrobial peptides-therapeutic agents and promising delivery vectors, Chem. Biol. Drug Des. 90 (2017) 1079–1093, https://doi.org/10.1111/cbdd.13031.

[14] Y. Jiang, Y. Chen, Z. Song, Z. Tan, J. Cheng, Recent advances in design of antimicrobial peptides and polypeptides toward clinical translation, Adv. Drug Deliv. Rev. 170 (2021) 261–280, https://doi.org/10.1016/j.addr.2020.12.016.

[15] M.H. Paulsen, M. Engqvist, D. Ausbacher, T. Anderssen, M.K. Langer, T. Haug, G. R. Morello, L.E. Liikanen, H.M. Blencke, J. Isaksson, E. Juskewitz, A. Bayer, M. B. Strøm, Amphipathic barbiturates as mimics of antimicrobial peptides and the marine natural products eusynstyelamides with activity against multi-resistant clinical isolates, J. Med. Chem. 64 (2021) 11395–11417, https://doi.org/10.1021/acs.jmedchem.1c00734.

[16] S.C. Park, C. Ko, H. Hyeon, M.K. Jang, D. Lee, Imaging and targeted antibacterial therapy using chimeric antimicrobial peptide micelles, ACS Appl. Mater. Interfaces 12 (2020) 54306–54315, https://doi.org/10.1021/acsami.0c13083.

[17] K. Forier, K. Raemdonck, S.C. De Smedt, J. Demeester, T. Coenye, K. Braeckmans, Lipid and polymer nanoparticles for drug delivery to bacterial biofilms, J. Control. Release 190 (2014) 607–623, https://doi.org/10.1016/j.jconrel.2014.03.055.

[18] J. Ndayishimiye, T. Kumeria, A. Popat, J.R. Falconer, M.A.T. Blaskovich, Nanomaterials: the new antimicrobial magic bullet, ACS Infect. Dis. 8 (2022) 693–712, https://doi.org/10.1021/acsinfecdis.1c00660.

[19] A.A. Aytekin, S. Tuncay Tanrıverdi, F. Aydın Köse, D. Kart, İ. Eroğlu, Ö. Özer, Propolis loaded liposomes: evaluation of antimicrobial and antioxidant activities, J. Liposome Res. 30 (2020) 107–116, https://doi.org/10.1080/08982104.2019.1599012.

[20] E. Bhatia, S. Sharma, K. Jadhav, R. Banerjee, Combinatorial liposomes of berberine and curcumin inhibit biofilm formation and intracellular methicillin resistant Staphylococcus aureus infections and associated inflammation, J. Mater. Chem. B 9 (2021) 864–875, https://doi.org/10.1039/D0TB02036B.

[21] L.M. Hemmingsen, B. Giordani, A.K. Pettersen, B. Vitali, P. Basnet, N. Škalko-Basnet, Liposomes-in-chitosan hydrogel boosts potential of chlorhexidine in biofilm eradication in vitro, Carbohydr. Polym. 262 (2021), 117939, https://doi.org/10.1016/j.carbpol.2021.117939.

[22] N. Škalko-Basnet, Ž. Vanić, Chapter 5 - lipid-based nanopharmaceuticals in antimicrobial therapy, in: R. Boukherroub, S. Szunerits, D. Drider (Eds.), Functionalized Nanomaterials for the Management of Microbial Infection, Elsevier, Boston, US, 2017, pp. 111–152.

[23] M. Cui, C. Wiraja, S.W.T. Chew, C. Xu, Nanodelivery systems for topical management of skin disorders, Mol. Pharm. 18 (2021) 491–505, https://doi.org/10.1021/acs.molpharmaceut.0c00154.

[24] M. Sguizzato, E. Esposito, R. Cortesi, Lipid-based nanosystems as a tool to overcome skin barrier, Int. J. Mol. Sci. 22 (2021) 8319, https://doi.org/10.3390/ijms22158319.

[25] Á. Martin-Serrano, R. Gómez, P. Ortega, F.J. de la Mata, Nanosystems as vehicles for the delivery of antimicrobial peptides (AMPs), Pharmaceutics 11 (2019) 448, https://doi.org/10.3390/pharmaceutics11090448.

[26] B. Giordani, P.E. Costantini, S. Fedi, M. Cappelletti, A. Abruzzo, C. Parolin, C. Foschi, G. Frisco, N. Calonghi, T. Cerchiara, F. Bigucci, B. Luppi, B. Vitali, Liposomes containing biosurfactants isolated from lactobacillus gasseri exert antibiofilm activity against methicillin resistant Staphylococcus aureus strains, Eur. J. Pharm. Biopharm. 139 (2019) 246–252, https://doi.org/10.1016/j.ejpb.2019.04.011.

[27] C. Bradford, R. Freeman, S.L. Percival, In vitro study of sustained antimicrobial activity of a new silver alginate dressing, J. Am. Col. Certif. Wound Spec. 1 (2009) 117–120, https://doi.org/10.1016/j.jcws.2009.09.001.

[28] R.K. Thapa, H.C. Winther-Larsen, D.B. Diep, H.H. Tønnesen, Preformulation studies on novel garvicin KS peptides for topical applications, Eur. J. Pharm. Sci. 151 (2020), 105333, https://doi.org/10.1016/j.ejps.2020.105333.

[29] M.H. Paulsen, M. Engqvist, D. Ausbacher, M.B. Strøm, A. Bayer, Efficient and scalable synthesis of alpha, alpha-disubstituted beta-amino amides, Org. Biomol. Chem. 14 (2016) 7570–7578, https://doi.org/10.1039/c6ob01219a.

[30] L.M. Hemmingsen, K. Julin, L. Ahsan, P. Basnet, M. Johannessen, N. Škalko-Basnet, Chitosomes-in-chitosan hydrogel for acute skin injuries: prevention and infection control, Mar. Drugs 19 (2021) 269, https://doi.org/10.3390/md19050269.

[31] Z. Palac, A. Engesland, G.E. Flaten, N. Škalko-Basnet, J. Filipović-Grčić, Ž. Vanić, Liposomes for (trans)dermal drug delivery: the skin-PVPA as a novel in vitro stratum corneum model in formulation development, J. Liposome Res. 24 (2014) 313–322, https://doi.org/10.3109/08982104.2014.899368.

[32] X. Liu, Z. Li, X. Wang, Y. Chen, F. Wu, K. Men, T. Xu, Y. Luo, L. Yang, Novel antimicrobial peptide-modified azithromycin-loaded liposomes against methicillin-resistant Staphylococcus aureus, Int. J. Nanomedicine 11 (2016) 6781–6794, https://doi.org/10.2147/ijn.S107107.

[33] J. Cauzzo, M. Nystad, A.M. Holsæter, P. Basnet, N. Škalko-Basnet, Following the fate of dye-containing liposomes in vitro, Int. J. Mol. Sci. 21 (2020) 4847, https://doi.org/10.3390/ijms21144847.

[34] R.F. Epand, B.P. Mowery, S.E. Lee, S.S. Stahl, R.I. Lehrer, S.H. Gellman, R. M. Epand, Dual mechanism of bacterial lethality for a cationic sequence-random copolymer that mimics host-defense antimicrobial peptides, J. Mol. Biol. 379 (2008) 38–50, https://doi.org/10.1016/j.jmb.2008.03.047.

[35] Y. Sun, W. Dong, L. Sun, L. Ma, D. Shang, Insights into the membrane interaction mechanism and antibacterial properties of chensinin-1b, Biomaterials 37 (2015) 299–311, https://doi.org/10.1016/j.biomaterials.2014.10.041.

[36] L. Lombardi, M.I. Stellato, R. Oliva, A. Falanga, M. Galdiero, L. Petraccone, G. D'Errico, A.De Santis, S. Galdiero, P.Del Vecchio, Antimicrobial peptides at work: interaction of myxinidin and its mutant WMR with lipid bilayers mimicking the P. aeruginosa and E. coli membranes, Sci. Rep. 7 (2017) 44425, https://doi.org/10.1038/srep44425.

[37] Y.Q. Xiong, K. Mukhopadhyay, M.R. Yeaman, J. Adler-Moore, A.S. Bayer, Functional interrelationships between cell membrane and Cell Wall in antimicrobial peptide-mediated killing of Staphylococcus aureus, Antimicrob. Agents Chemother. 49 (2005) 3114–3121, https://doi.org/10.1128/AAC.49.8.3114-3121.2005.

[38] S. Kobayashi, K. Takeshima, C.B. Park, S.C. Kim, K. Matsuzaki, Interactions of the novel antimicrobial peptide buforin 2 with lipid bilayers: proline as a translocation promoting factor, Biochemistry 39 (2000) 8648–8654, https://doi.org/10.1021/bi0004549.

[39] B. Orioni, G. Bocchinfuso, J.Y. Kim, A. Palleschi, G. Grande, S. Bobone, Y. Park, J. I. Kim, K.S. Hahm, L. Stella, Membrane perturbation by the antimicrobial peptide PMAP-23: a fluorescence and molecular dynamics study, Biochim. Biophys. Acta Biomembr. 1788 (2009) 1523–1533, https://doi.org/10.1016/j.bbamem.2009.04.013.

[40] N. Yamamoto, A. Tamura, Designed low amphipathic peptides with α-helical propensity exhibiting antimicrobial activity via a lipid domain formation mechanism, Peptides 31 (2010) 794–805, https://doi.org/10.1016/j.peptides.2010.01.006.

[41] EUCAST—the European Committee on Antimicrobial Susceptibility Testing, EUCAST Reading Guide for Broth Microdilution, 2020.

[42] A. Zajmi, N.M. Hashim, M.I. Noordin, S.A.M. Khalifa, F. Ramli, H. Mohd Ali, H. R. El-Seedi, Ultrastructural study on the antibacterial activity of artonin E versus streptomycin against Staphylococcus aureus strains, PLoS One 10 (2015), e0128157, https://doi.org/10.1371/journal.pone.0128157.

[43] S. Ron-Doitch, B. Sawodny, A. Kuhbacher, M.M.N. David, A. Samanta, J. Phopase, A. Burger-Kentischer, M. Griffith, G. Golomb, S. Rupp, Reduced cytotoxicity and enhanced bioactivity of cationic antimicrobial peptides liposomes in cell cultures and 3D epidermis model against HSV, J. Control. Release 229 (2016) 163–171, https://doi.org/10.1016/j.jconrel.2016.03.025.

[44] A.M. Robinson, M. Bannister, J.E. Creeth, M.N. Jones, The interaction of phospholipid liposomes with mixed bacterial biofilms and their use in the delivery of bactericide, Colloids Surf. A Physicochem. Eng. Asp. 186 (2001) 43–53, https://doi.org/10.1016/S0927-7757(01)00481-2.

[45] M. Elmowafy, Skin penetration/permeation success determinants of nanocarriers: pursuit of a perfect formulation, Colloids Surf. B: Biointerfaces 203 (2021), 111748, https://doi.org/10.1016/j.colsurfb.2021.111748.

[46] Z. Rukavina, M. Šegvić Klarić, J. Filipović-Grčić, J. Lovrić, Ž. Vanić, Azithromycin-loaded liposomes for enhanced topical treatment of methicillin-resistant staphyloccocus aureus (MRSA) infections, Int. J. Pharm. 553 (2018) 109–119, https://doi.org/10.1016/j.ijpharm.2018.10.024.

[47] M.J. Choi, H.I. Maibach, Liposomes and niosomes as topical drug delivery systems, Skin Pharmacol. Physiol. 18 (2005) 209–219, https://doi.org/10.1159/000086666.

[48] J. Hurler, O.A. Berg, M. Skar, A.H. Conradi, P.J. Johnsen, N. Škalko-Basnet, Improved burns therapy: liposomes-in-hydrogel delivery system for mupirocin, J. Pharm. Sci. 101 (2012) 3906–3915, https://doi.org/10.1002/jps.23260.

[49] M. Danaei, M. Dehghankhold, S. Ataei, F.Hasanzadeh Davarani, R. Javanmard, A. Dokhani, S. Khorasani, M.R. Mozafari, Impact of particle size and polydispersity index on the clinical applications of lipidic nanocarrier systems, Pharmaceutics 10 (2018) 57, https://doi.org/10.3390/pharmaceutics10020057.

[50] Z. Rukavina, Ž. Vanić, Current trends in development of liposomes for targeting bacterial biofilms, Pharmaceutics 8 (2016) 18, https://doi.org/10.3390/pharmaceutics8020018.

[51] H.J. Kim, E.L.M. Gias, M.N. Jones, The adsorption of cationic liposomes to Staphylococcus aureus biofilms, Colloids Surf. A Physicochem. Eng. Asp. 149 (1999) 561–570, https://doi.org/10.1016/S0927-7757(98)00765-1.

[52] S. Sandreschi, A.M. Piras, G. Batoni, F. Chiellini, Perspectives on polymeric nanostructures for the therapeutic application of antimicrobial peptides, Nanomedicine 11 (2016) 1729–1744, https://doi.org/10.2217/nnm-2016-0057.

[53] L.A. Wallace, L. Gwynne, T. Jenkins, Challenges and opportunities of pH in chronic wounds, Ther. Deliv. 10 (2019) 719–735, https://doi.org/10.4155/tde-2019-0066.

[54] N. Mookherjee, M.A. Anderson, H.P. Haagsman, D.J. Davidson, Antimicrobial host defence peptides: functions and clinical potential, Nat. Rev. Drug Discov. 19 (2020) 311–332, https://doi.org/10.1038/s41573-019-0058-8.

[55] A. Alghalayini, A. Garcia, T. Berry, C.G. Cranfield, The use of tethered bilayer lipid membranes to identify the mechanisms of antimicrobial peptide interactions with lipid bilayers, Antibiotics 8 (2019) 12, https://doi.org/10.3390/antibiotics8010012.
[56] L.M. Hemmingsen, N. Škalko-Basnet, M.W. Jøraholmen, The expanded role of chitosan in localized antimicrobial therapy, Mar. Drugs 19 (2021) 697, https://doi.org/10.3390/md19120697.
[57] Y. Liu, Y. Li, L. Shi, Controlled drug delivery systems in eradicating bacterial biofilm-associated infections, J. Control. Release 329 (2021) 1102–1116, https://doi.org/10.1016/j.jconrel.2020.10.038.
[58] P.S. Korrapati, K. Karthikeyan, A. Satish, V.R. Krishnaswamy, J.R. Venugopal, S. Ramakrishna, Recent advancements in nanotechnological strategies in selection, design and delivery of biomolecules for skin regeneration, Mater. Sci. Eng. C 67 (2016) 747–765, https://doi.org/10.1016/j.msec.2016.05.074.
[59] K. Shanmugapriya, H.W. Kang, Engineering pharmaceutical nanocarriers for photodynamic therapy on wound healing: review, Mater. Sci. Eng. C 105 (2019), 110110, https://doi.org/10.1016/j.msec.2019.110110.
[60] P. Méndez-Samperio, Peptidomimetics as a new generation of antimicrobial agents: current progress, Infect. Drug Resist. 7 (2014) 229–237, https://doi.org/10.2147/IDR.S49229.
[61] S. Ternullo, P. Basnet, A.M. Holsæter, G.E. Flaten, L. de Weerd, N. Škalko-Basnet, Deformable liposomes for skin therapy with human epidermal growth factor: the effect of liposomal surface charge, Eur. J. Pharm. Sci. 125 (2018) 163–171, https://doi.org/10.1016/j.ejps.2018.10.005.
[62] H.N. Wilkinson, M.J. Hardman, Wound healing: cellular mechanisms and pathological outcomes, Open Biol. 10 (2020), 200223, https://doi.org/10.1098/rsob.200223.
[63] J. Larouche, S. Sheoran, K. Maruyama, M.M. Martino, Immune regulation of skin wound healing: mechanisms and novel therapeutic targets, Adv. Wound Care 7 (2018) 209–231, https://doi.org/10.1089/wound.2017.0761.
[64] K. Las Heras, M. Igartua, E. Santos-Vizcaino, R.M. Hernandez, Chronic wounds: current status, available strategies and emerging therapeutic solutions, J. Control. Release 328 (2020) 532–550, https://doi.org/10.1016/j.jconrel.2020.09.039.
[65] S. Ellis, E.J. Lin, D. Tartar, Immunology of wound healing, Curr. Dermatol. Rep. 7 (2018) 350–358, https://doi.org/10.1007/s13671-018-0234-9.
[66] A. Soneja, M. Drews, T. Malinski, Role of nitric oxide, nitroxidative and oxidative stress in wound healing, Pharmacol. Rep. 57 (Suppl) (2005) 108–119.
[67] M. Ahn, P. Gunasekaran, G. Rajasekaran, E.Y. Kim, S.J. Lee, G. Bang, K. Cho, J. K. Hyun, H.J. Lee, Y.H. Jeon, N.H. Kim, E.K. Ryu, S.Y. Shin, J.K. Bang, Pyrazole derived ultra-short antimicrobial peptidomimetics with potent anti-biofilm activity, Eur. J. Med. Chem. 125 (2017) 551–564, https://doi.org/10.1016/j.ejmech.2016.09.071.
[68] B. Giordani, P. Basnet, E. Mishchenko, B. Luppi, N. Škalko-Basnet, Utilizing liposomal quercetin and gallic acid in localized treatment of vaginal Candida infections, Pharmaceutics 12 (2019) 9, https://doi.org/10.3390/pharmaceutics12010009.
[69] M.Y. Lee, S.C. Park, M. Jung, M.K. Shin, H.L. Kang, S.C. Baik, G.W. Cheong, M. K. Jang, W.K. Lee, Cell-selectivity of tryptophan and tyrosine in amphiphilic alpha-helical antimicrobial peptides against drug-resistant bacteria, Biochem. Biophys. Res. Commun. 505 (2018) 478–484, https://doi.org/10.1016/j.bbrc.2018.09.095.
[70] M.B. Strøm, B.E. Haug, M.L. Skar, W. Stensen, T. Stiberg, J.S. Svendsen, The pharmacophore of short cationic antibacterial peptides, J. Med. Chem. 46 (2003) 1567–1570, https://doi.org/10.1021/jm0340039.
[71] C. Mazzuca, L. Stella, M. Venanzi, F. Formaggio, C. Toniolo, B. Pispisa, Mechanism of membrane activity of the antibiotic trichogin GA IV: a two-state transition controlled by peptide concentration, Biophys. J. 88 (2005) 3411–3421, https://doi.org/10.1529/biophysj.104.056077.
[72] A. Patrzykat, L. Friedrich Carol, L. Zhang, V. Mendoza, R.E.W. Hancock, Sublethal concentrations of pleurocidin-derived antimicrobial peptides inhibit macromolecular synthesis in Escherichia coli, Antimicrob. Agents Chemother. 46 (2002) 605–614, https://doi.org/10.1128/AAC.46.3.605-614.2002.
[73] A.F. Cardona, S.E. Wilson, Skin and soft-tissue infections: a critical review and the role of telavancin in their treatment, Clin. Infect. Dis. 61 (2015) S69–S78, https://doi.org/10.1093/cid/civ528.
[74] G. Daeschlein, Antimicrobial and antiseptic strategies in wound management, Int. Wound J. 10 (2013) 9–14, https://doi.org/10.1111/iwj.12175.
[75] K. Vowden, P. Vowden, Understanding exudate management and the role of exudate in the healing process, Br. J. Community Nurs. 8 (2003) S4–S13, https://doi.org/10.12968/bjcn.2003.8.Sup5.12607.
[76] P. Cardoso, H. Glossop, T.G. Meikle, A. Aburto-Medina, C.E. Conn, V. Sarojini, C. Valery, Molecular engineering of antimicrobial peptides: microbial targets, peptide motifs and translation opportunities, Biophys. Rev. 13 (2021) 35–69, https://doi.org/10.1007/s12551-021-00784-y.
[77] T.F.C. Mah, G.A. O'Toole, Mechanisms of biofilm resistance to antimicrobial agents, Trends Microbiol. 9 (2001) 34–39, https://doi.org/10.1016/S0966-842X(00)01913-2.
[78] L.R. Mulcahy, V.M. Isabella, K. Lewis, Pseudomonas aeruginosa biofilms in disease, Microb. Ecol. 68 (2014) 1–12, https://doi.org/10.1007/s00248-013-0297-x.
[79] M. Okshevsky, R.L. Meyer, The role of extracellular DNA in the establishment, maintenance and perpetuation of bacterial biofilms, Crit. Rev. Microbiol. 41 (2015) 341–352, https://doi.org/10.3109/1040841X.2013.841639.
[80] M.E. van Gent, M. Ali, P.H. Nibbering, S.N. Kłodzińska, Current advances in lipid and polymeric antimicrobial peptide delivery systems and coatings for the prevention and treatment of bacterial infections, Pharmaceutics 13 (2021) 1840, https://doi.org/10.3390/pharmaceutics13111840.